Fisheries and Oceans Canada | Pêches et Océans Canada
Ecosystems and Oceans Science | Sciences des écosystèmes et des océans

Canadian Science Advisory Secretariat (CSAS)

Research Document 2023/086

Quebec Region

Adjustment of a Bayesian Surplus Production Model for Northern Shrimp for Stocks in the Gulf of St. Lawrence

Andrew Smith and Hugo Bourdages

Fisheries and Oceans Canada
Maurice Lamontagne Institute
850 route de la Mer
Mont-Joli, Quebec G5H 3Z4

October 2024

Canada

Foreword

This series documents the scientific basis for the evaluation of aquatic resources and ecosystems in Canada. As such, it addresses the issues of the day in the time frames required and the documents it contains are not intended as definitive statements on the subjects addressed but rather as progress reports on ongoing investigations.

Published by:

Fisheries and Oceans Canada
Canadian Science Advisory Secretariat
200 Kent Street
Ottawa ON K1A 0E6

http://www.dfo-mpo.gc.ca/csas-sccs/
csas-sccs@dfo-mpo.gc.ca

ISSN 1919-5044
ISBN 978-0-660-73499-6 Cat. No. Fs70-5/2023-086E-PDF

Correct citation for this publication:

Smith, A. and Bourdages, H. 2024. Adjustment of a Bayesian Surplus Production Model for Northern Shrimp for Stocks in Gulf of St. Lawrence. DFO Can. Sci. Advis. Sec. Res. Doc. 2023/086. iv + 56 p.

Aussi disponible en français :

Smith, A. et Bourdages, H. 2024. Ajustement d'un modèle bayésien de production excédentaire pour la crevette nordique des stocks du golfe du Saint-Laurent. Secr. can. des avis sci. du MPO. Doc. de rech. 2023/086. iv + 57 p.

TABLE OF CONTENTS

ABSTRACT

As part of the review of the precautionary approach for northern shrimp in the Estuary and northern Gulf of St. Lawrence (ENGSL), a Bayesian, state-space, surplus production model was fit to commercial landings and the biomass index for each of the four stocks.

This document describes the methods used to fit the Bayesian surplus production model to biomass data for the northern shrimp stocks in the ENGSL. According to the results obtained, this model could be useful for assessing stock status and for revising the precautionary approach. The results presented here are consistent with the findings of the previous assessment and show that the Esquiman, Anticosti and Sept-Iles stocks have been declining for several years, with biomass values in 2022 falling to the lowest levels observed since 1990. The results also show that the Estuary stock is currently stable with high biomass values.

INTRODUCTION

Northern shrimp (*Pandalus borealis*) is one of the most important commercial species in Canadian waters from an economic standpoint. An initial precautionary approach for the four northern shrimp stocks in the Estuary and Gulf of St. Lawrence (ENGSL) was adopted in 2012 (DFO 2011). However, during the last stock assessment, conducted in the winter of 2022 (DFO 2022), it was concluded that the precautionary approach should be revised before the next assessment. This revision was justified because ecosystem conditions have changed since the precautionary approach was developed in the early 2010s and because of the bias in the principal stock status indicator.

Until now, no stock assessment model was available for these stocks that could estimate trends in population abundance and fishing pressure on these stocks. To overcome the limitations inherent in the use of empirical reference points described above, a new assessment model is proposed to

1. estimate the population biomass;
2. determine reference points that are consistent with the precautionary approach;
3. estimate the exploitation rate;
4. take changing environmental conditions into account; and
5. make projections.

This document presents the results obtained from fitting a Bayesian surplus production model (SPM) to biomass of the ENGSL northern shrimp stocks. This stock assessment model uses commercial landings data and an index of total biomass. This type of model (SPM) is routinely used in stock assessments.

The model fitting results can be used to estimate several biological parameters that describe the dynamics of these stocks. To assess the stability of the model in relation to our assumptions and the different sources of uncertainty, we examined several versions of the model for each stock in order to determine a model formulation that was most appropriate in the context of the assessment of the status of northern shrimp stocks in the ENGSL. The results obtained can be used in development of the precautionary approach.

METHODS

DATA USED

Fitting SPM requires a time series of total catch (landings) data and a time series of biomass index values representing the exploitable component of the stock. Annual landings data were used by stock began in 1982 (Table 1, Figure 1). The estimates of total biomass derived from the DFO research survey (conducted annually in August since 1990) were used to represent the exploitable component of the stocks (Table 2, Figure 2). The description of these data and the methods used to acquire and process these data are described in Bourdages et al. (2022). In addition, we used updated indicator data based on the assessment units that Bourdages et al. (2023) in order to have a better match between the spatial scales of the management units and biological units of these stocks.

For the base models, we chose to start all the time series in 1990 to take into account the availability of biomass index. Sensitivity tests (described below) were conducted to assess the impact of including landings data from 1982 to 1989. The Estuary stock is a special case. We

opted to use only data beginning in 2008 because the area covered by the research survey was expanded in 2008 to cover shallower strata where shrimp are quite abundant. Sensitivity tests will also conducted to examine the effect of including and excluding landings data from before 2008.

SURPLUS PRODUCTION MODEL

The SPM is based on the logistic growth of a discrete population (Verhulst 1838). The effects of recruitment, growth and mortality are pooled together to describe the productivity of a population in its environment as well as trends in its biomass. The model assumes that a population is productive enough to persist over time by producing more recruits than the environment has the capacity to support. The maximum sustainable yield (MSY) is the maximum amount of biomass that can on average be removed from a fishery stock under existing environmental conditions, without affecting the stock productivity. It is recognized that this theoretical value should be considered a limit and not a target (Pauly and Froese 2021).

The Schaefer-type (SPM) (Schaefer 1954) was formulated in a Bayesian state-space framework (Meyer and Millar 1999). State-space models make it possible to estimate process error, that is, stochasticity in the population dynamics, as well as observation error associated with the biomass index. This approach is considered by many to be the best practice for stock assessment (Aeberherd et al. 2018; Punt 2023).

The stochastic form of the process equation is:

$$P_t = \left(P_{t-1} + rP_{t-1}(1 - P_{t-1}) - \frac{C_{t-1}}{K}\right) e^{\eta_t}$$

where r is the intrinsic rate of population increase, which encompasses all growth, recruitment and natural mortality processes; K is the carrying capacity of the system; C_t is the sum of catches in year t estimated from the observed values using a log normal distribution with a CV of 0.1; P_t is the ratio of exploitable biomass (B) to carrying capacity in year t ($P_t = B_t/K$); η_t is the process error $\eta_t \sim N(0,\sigma_\eta^2)$ with process variance σ_η^2. The model estimates biomass as a proportion of carrying capacity to enhance the sampling of parameter space and minimize autocorrelation between each state and K (Meyer and Millar 1999). This also ensures that process error and observation error are treated separately from uncertainty in estimates of r and K (Froese *et al.* 2017; Pedersen and Berg 2017; Winker *et al.* 2018).

An observation equation is used to link biomass (B_t) and the observations from the bottom trawl survey.

$$I_t = (qB_t)\, e^{\varepsilon_t}$$

where I_t is the biomass index in year t; q is the catchability coefficient and ε_t is observation error associated with the biomass index $\varepsilon_t \sim N(0,\sigma_{\varepsilon,t}^2)$ with variance $\sigma_{\varepsilon,t}^2$ which is composed of a minimum variance, fixed at $0.2^2\ \sigma_{fix}^2$ (Winker *et al.* 2018) and an estimated portion $\sigma_{est,t}^2$.

With the Bayesian SPM approach, it is possible to determine the probability distribution (posterior distributions, or “posteriors”) of the different possible values of the parameters to be estimated. Existing knowledge (prior distributions, or “priors”) of the parameters, the observed data and the likelihood function are combined to generate the posterior distributions. This approach allows uncertainty to be included and propagated to the observations, biomass trends and the productivity of a stock when its status is being assessed (Winker et al. 2018).

The biomasses trajectories were calculated using prior estimates for K, r, q and biomass as a proportion of K in the first year of the time series of catches (B_1/K), as well as process error

variance and observation error variance, $\sigma^2_{\varepsilon,t}$ and $\sigma^2_{est,t}$ respectively (Table 3). The parameters estimated by the SPM are as follows: r, K, q, B_1/K, σ^2_η, $\sigma^2_{est,t}$, C_t and P_t.

Annual biomasses (B_t) and the annual exploitation rate (F_t) are calculated along with reference points based on the maximum sustainable yield (MSY): the exploitation rate that would maintain the MSY (F_{MSY}), biomass at MSY (B_{MSY}) and B_t/B_{MSY} and F_t/F_{MSY}. These values are calculated using the following equations:

$$B_{MSY} = \frac{K}{2}$$

$$F_{MSY} = \frac{r}{2}$$

$$MSY = F_{MSY} \times B_{MSY} = \frac{rK}{4}$$

$$B_t = KP_t$$

$$F_t = \frac{C_t}{B_t}$$

Model were fit using the open-source stock assessment platform JABBA ("Just another Bayesian Biomass Assessment"; Winker et al. 2018, 2020). JABBA enables the user to prepare data to be used to fit a generalized Bayesian state-space SPM, format model outputs, conduct diagnostic tests and generate plots.

More specifically, JABBA prepares the input to be executed with JAGS software ("Just Another Gibbs Sampler": Plummer 2003), which is written in C++. JAGS uses Markov Chain Monte Carlo simulations (MCMC) using the Gibbs sampling algorithm, to make Bayesian inferences. JABBA, through JAGS, compiles the model using code generated by R2jags (Su and Yajima 2012). All code used to perform the analyses and generate plots was written in R (R Core Team 2022; version 4.1.3).

MCMC sampling of the posterior distributions of the parameters was carried out using 3 chains, 30,000 iterations and an adaptation period of 5,000 iterations. Samples were thinned to every fifth iteration to reduce the possibility of autocorrelation within the series. Therefore, the final number of samples in each posterior distribution was (30,000 – 5,000)/5 *3 = 15,000 samples per parameter.

PRIOR DISTRIBUTION

In a Bayesian modelling framework, prior distributions, are provided for each parameter in the model. Together, with the observed data and the likelihood function (Winker et al. 2018), these prior distributions are updated to produce posterior distributions. This differs from classical modelling approaches in that the likelihood values are weighted by the priors to provide the posteriors. One of the advantages of this probabilistic methodology is that it allows prior knowledge to be used when the required information is unavailable or uncertain.

Priors can be based on knowledge acquired in previous studies, from research on different stocks of the same or similar species, from relationships based on ecological laws and theories, and from expert opinion (Krushke 2021, Pauly and Froese 2021). JABBA allows the user to select the form and scale for certain parameters (Table 3).

Intrinsic rate of increase (*r*)

The prior distribution for *r* for each of the four stocks followed a lognormal distribution with a mean of 0.58 and a standard deviation of 0.5 on the log scale. The mean of 0.58 was based on an analysis of several shrimp stock assessments described on the SeaLifeBase website (Palomares et al. 2023). This distribution is similar to *r* values estimated by Bayesian SPMs used to assess other northern shrimp stocks, specifically the Barents Sea, North Sea and West Greenland stocks (Hvingel 2015, 2019; Hvingel and Kingsley 2001), as well as other species of shrimp and decapods with medium to high resilience (Caddy 2004, Zhou et al. 2009, ICES 2015).

Carrying capacity (*K*)

The prior distribution for *K* for each of the four stocks was established by using information from the time series of catches as well as our knowledge about the productivity (*r*) of this species. We assumed that

1. the *K* for each stock should be greater than the maximum catch in the respective series;
2. that the maximum yield for each stock depends on its productivity; and
3. that catches account for a larger proportion of *K* in strongly depleted stocks than in healthy stocks (Froese et al. 2017).

We therefore chose a range of values corresponding from 2 to 12 times the highest catch value for each stock. Each of these values was divided by our prior for *r*, that is, 0.58. The default prior distribution for *K* in JABBA is 8 times the maximum catch with a standard deviation of ~0.83 (CV = 1). These ranges of values are transformed by JABBA into log-normal distributions. JABBA penalizes the likelihood of values of $K < 0.01$ and $K > 10^{10}$ by default.

Catchability coefficient of the biomass index (*q*)

Although a total biomass index is used, we chose a non-informative distribution for *q* based on the recommendations of Punt and Hilborn (1997). The default in JABBA is a uniform distribution, that is, a range from 10^{-30} to 1,000. JABBA penalizes the likelihood of values diverging from these bounds, by default.

Initial depletion in the first year of the series (B_1/K)

We followed the recommendations of the ICES WKLIFE IV and V working groups (ICES 2015) and those of Froese et al. (2017) for the specification of B_1/K by taking into account the stock's exploitation history and its assumed level of depletion. Although stock exploitation was low prior to 1990, a regime shift occurred in the ENGSL in the late 1980s, from a regime dominated by the main predators of shrimp to one dominated by other species. Given this pattern, we assumed that the ENGSL shrimp stocks were at fairly low levels in relation to carrying capacity. Furthermore, we assumed that the B_1/K for each stock could be described by a beta distribution with a mean value of 0.2 and a CV of 0.25. We assumed, with this distribution, that biomass values were low relative to carrying capacity in 1990. The Estuary series began in 2008, productive period for shrimp stocks given lower abundance of predators. In this case, we assumed that the B_1/K for the stock could be described by a beta distribution with a mean value of 0.5 and a CV of 0.25. The likelihood of P_t is penalized for values <0.01 and >1.3 by default.

Process and observation error variance

We followed the approach developed by Meyer and Millar (1999) and assigned non-informative prior distributions to the process error and the estimated portion of the observation error variance parameters (i.e., an inverse gamma distribution (0.001, 0.001). This distribution is almost uniform on a log scale. The minimum variance (σ_{fix}) was set at 0.2 in keeping with the JABBA authors' recommendations regarding plausible observation error values and the partitioning of process and observation error (Winker et al. 2018). Annual catches are also estimated in the model and are taken from a log-normal distribution with a CV of 0.1 despite the assumption that the catch monitoring system for shrimp is well managed.

DIAGNOSTICS

The consistency and stability of the model outputs was evaluated in several ways. Model convergence was evaluated with the potential scale reduction statistic "*R-hat*" (Gelman and Rubin 1992), which is a weighted mean of the variance between and within each MCMC chain. This statistic is automatically calculated in JABBA using the wrapper function jags() from the library R2jags (Winker et al. 2018). Values below 1.1 provide evidence of convergence in the outputs. A more robust variant of *R-hat* was also calculated and used to validate convergence of the models (Vehtari et al. 2021). Given the large number of parameters that need to be estimated in hierarchical state-space models, we followed the recommendations of Kruschke (2021) by ensuring that all the *R-hat* values (n = 3,123) for each model were below 1.1 before conducting other diagnostic tests (Table 4).

Model fit was assessed in each case by means of several statistics and plots generated automatically by JABBA (Carvalho et al. 2021; Winker et al. 2018). The log-normal residuals of the observed and predicted biomass index values were first inspected visually to check for temporal trends. The root mean square error (RMSE), the standard deviation of the normalized residuals (SDNR) and the Wald-Wolfowitz residual runs test were also calculated.

The quality of the posterior distributions of certain key parameters as well as the influence of the data in relation to the priors on the posterior distributions is evaluated using the "prior-posterior mean ratio" and the "prior posterior variance ratio" (PPMR and PPVR respectively).

The stability of the estimates and the model's consistency in relation to our assumptions as well as its capacity to simulate and predict values similar to our observations was also evaluated. We started by inspecting the process error deviates for temporal trends. We ensured that the simulated values of the predictive posterior distribution could reproduce biomass values that included our observations ("posterior predictive check PPD").

Finally, we performed retrospective analyses spanning four years to see whether the estimates would remain stable after more information was added. We inspected these figures for evidence of extreme biases and that the estimates did not exceed the confidence intervals of the full model (all years included). Mohn's rho statistic can be used to measure the severity of retrospective patterns.

SENSITIVITY ANALYSIS

A crucial step in Bayesian modeling is to assess the stability in parameter estimation due to the inherent uncertainty of our assumptions (Punt 2023). We therefore compared the results obtained from our base models using a series of sensitivity tests (Table 9).

Given that stock productivity and/or the systems' carrying capacity could have changed over time (e.g., temporal variation in recruitment, natural mortality, growth, available thermal niche), we varied the means and variances of the prior distributions of *r* and *K*. We analyzed scenarios

with lower (s1; r = 0.3) and higher (s2; r = 0.9) prior values for r; a scenario with a smaller and therefore more informative standard deviation (s3; r log SD = 0.1); and a scenario where r had a larger and therefore less informative standard deviation (s4; r log SD = 1.0).

Similarly, we tested scenarios with lower (s5; range of 2 to 6 times maximum catch/r) and higher (s6; range of 8 to 12 times maximum catch/r) prior values for K, and a scenario where the CV of K is about double that in the base models, that is, a CV of 0.83 versus a CV of 0.45 (s7; 2 to 24 times maximum catch/r).

Given that many species reach production equilibrium at a B_{MSY}/K value of about 0.4 (Thorson et al. 2012, Punt *et al.* 2014), we tested a Pella-Tomlinson SPM formulation in JABBA by setting the B_{MSY}/K parameter with a CV of 0.3 (s8).

It is recognized that the value of the initial relative biomass (B_1/K) can have a considerable effect on the results of several stock assessment methods (Boudreau and Duplisea 2022) and can produce biased advice if the model is not suitable for describing the dynamics of the system. We therefore developed scenarios where B_1/K is equal to 0.5 and 0.7 (s9 and s10, respectively); for the Estuary, these values were a B_1/K of 0.2 a B_1/K of 0.7 in the s9 and s10 scenarios respectively.

Using an approach similar to that of Bailey (2012), who applied a Schaefer Bayesian state-space SPM to the 3LNO, 3Ps and 2J3KL American plaice stocks—similar in concept to retrospective analyses—we developed scenarios incorporating information from different periods of time in the model. The series of biomass index values was set to begin in 1990 and the series of catches, in 1982. Since JABBA allows missing values in series of indices, we created a scenario incorporating the catches from 1982 to 2022 (s11). Two scenarios (s12 and s13) were used to analyze the periods corresponding to the rising and descending trends observed in the time series of total biomass values (1990–2005 and 2005–2022, respectively).

For all the sensitivity tests, we compared the estimates of posterior distributions (medians and 95% CI) for the key model parameters (K, r, q, B_1/K, process error, sigma2_proc and sigma2_obs) and the derived quantities (MSY, B_{MSY}, F_{MSY}, B_{2022}/B_{MSY} and F_{2022}/F_{MSY}) with the base model.

COMPARISON WITH OTHER TYPES OF MODELS

Like Bouch et al. (2020), Pons et al. (2020) and Cousido-Rocha et al. (2022), we compared the JABBA results with those of other stock assessment models that apply the surplus production paradigm. Specifically, we fitted the SPM formulation of SPICT (Pederson and Berg 2017) and the latest version of CMSY++ (Froese et al. 2017). The latter fits a model based solely on catches, but provides a BSM (Bayesian Schaefer Model) fit if a biomass index is provided. The SPM formulations, algorithms and modelling frameworks for these models differ from those in JABBA, but the parameterization of the models and the prior distributions provided were essentially the same.

For the comparisons with other types of models, we compared the posterior estimates (medians and 95% CI) for the key model parameters (K, r, q, B_1/K, process error, sigma2_proc and sigma2_obs) and the derived quantities (MSY, B_{MSY}, F_{MSY}, B_{2022}/B_{MSY} and F_{2022}/F_{MSY}) with the base model.

RESULTS

The Bayesian surplus production model (SPM) was fit to the data from each stock, that is, the Esquiman, Anticosti, Sept-Iles and Estuary. None of the base models showed problems of

convergence and the MCMC chains sampled the parameter space well (Table 4). The results of the posterior distributions for each stock are presented in Tables 5 to 8 and Figures 3, 11, 19 and 27, respectively. While taking northern shrimp ecology and the sampling plan for the bottom trawl survey, which provided the observed biomass index into account, the results show that parameter estimates for *r, K,* B_1/K and *q* for each of these stocks is plausible,. Furthermore, the levels of annual process and observation variance found for each stock are reasonable and fall within the range of values where SPMs perform adequately (Thorson et al. 2014; Winker et al. 2018).

MODEL FITTING

Esquiman

The model showed a good fit to the data for the Esquiman stock (RMSE = 29.4; SDNR = 0.90). The observed values for the annual biomass index fell within the posterior distribution and the predictive posterior distribution (Figure 4). The analysis of residuals showed a slight tendency to underestimate biomass before 2003 and to overestimate biomass after 2003. Only the residual for 2003 appeared problematic in terms of model fit (Figure 5).

The absolute and relative trends in biomass at MSY and the stock exploitation rate are shown in Figure 6. The results of the retrospective analyses show that biomass tended to be overestimated when information is removed from the model. Therefore, the biomass estimates in the global model should be viewed with caution. The estimates from each sub-model nonetheless fell within the confidence intervals of the global model (Figure 7). Although the process error deviates (Figure 8) remained close to 0 throughout the time series, a slight negative trend was found after the early 2010s. This additional variation, which is not explained by the deterministic part of the model, could be due to variability in natural processes such as changes in recruitment and natural mortality, or variation in stock exploitation rates. In 2022, the stock biomass would be below the value for B_{MSY} and above the value for F_{MSY} (Figures 6, 9–10).

Anticosti

The model fit the Anticosti stock data well (RMSE = 31.3; SDNR = 0.93). The observed values for the annual biomass index fell within the posterior distribution and the predictive posterior distribution (Figure 12). Analysis of the residuals showed no particular temporal trend (Figure 13).

The absolute and relative trends in biomass at MSY and the stock exploitation rate are shown in Figure 14. The results of the retrospective analyses showed a slight tendency to overestimate biomass. Therefore, the biomass values in the global model should be viewed with caution. The estimates from each sub-model nonetheless fell within the confidence intervals the global model (Figure 15). No particular temporal trend was found in the process error deviates (Figure 16), but it had been slightly negative for the past few years. This additional variation not explained by the deterministic part of the model could be due to variability in natural processes such as changes in recruitment and natural mortality, or variation in stock exploitation rates. In 2022, the stock biomass would be below the value for B_{MSY} and above the value for F_{MSY} (Figures 14, 17–18).

Sept-Iles

The model fit the Sept-Iles stock data well (RMSE = 23.1; SDNR = 0.90). The observed values for the annual biomass index fell within the posterior distribution and the predictive posterior

distribution (Figure 20). Analysis of the residuals did not reveal any particular temporal trends but, as was the case for the Esquiman stock, a slight downward trend was found before 2003 and a slight upward trend was found from 2010 to 2020 (Figure 21).

Trends in biomass and exploitation rates are shown in Figure 22 in both absolute terms (also showing the respective values corresponding to MSY) and relative terms against B_{MSY} and F_{MSY} respectively. The results of the retrospective analyses showed the model's tendency to overestimate biomass, particularly the sub-model, which used two fewer years of information. Therefore, the biomass values provided by the global model must be viewed with caution. However, the overall trends revealed by the sub-models were similar to those provided by the global model, with values remaining largely within the confidence intervals (Figure 23). No particular temporal trend was found in the process error deviates values (Figure 24), although a slight upward trend occurred between 1994 and 2003 and a downward one in recent years (2014–2022). This additional variation not explained by the deterministic portion of the model could be due to variability in natural processes such as changes in recruitment and natural mortality, or variation in the stock exploitation rates. In 2022, stock biomass would be below the value for B_{MSY} and above that for F_{MSY} (Figures 22 and 25–26).

Estuary

The model's fit to the data was more problematic for the Estuary stock than for the other stocks (RMSE = 70.4; SDNR = 0.97), perhaps because of the shorter time series and lower exploitation rates for this stock. Consequently, the parameters were estimated using less information. The extreme values obtained for the biomass index in 2017, 2020 and 2022 probably also contributed to model fitting problems (Figure 2). The 2022 biomass index value used as model input was heavily influenced by two extremely large trawl tows but, despite this issue, the observed values for the annual biomass index fell within the posterior and predictive posterior distributions (Figure 28). In spite of the RMSE of 70.4%, residual analysis showed no particular temporal trends (Figure 29).

Trends in biomass and exploitation rates are shown in Figure 30 in both absolute terms (also showing the respective values corresponding to MSY) and relative terms against B_{MSY} and F_{MSY} respectively. The results of the retrospective analyses demonstrated that biomass tended to be underestimated when information was removed from the global model. This is probably due to the extreme positive value in 2022. These patterns will have to be reassessed with additional years of information. Nevertheless, the estimates of each sub-model fell within the confidence intervals for the global model (Figure 31). The process error deviates showed no particular temporal trends, although a slight positive trend could be seen in the last few years (Figure 32). In 2022, the stock biomass would be greater than B_{MSY}, while the exploitation rate was less than F_{MSY} (Figures 30, 33–34).

SENSITIVITY ANALYSIS

We carried out an extensive series of sensitivity analyses to test our assumptions on the intrinsic rate of increase, the carrying capacity and the constancy of productivity regimes over time. Changes in our underlying assumptions did not produce results that differed appreciably from those obtained from our base models, given that the sensitivity analyses produced parameter estimates similar to those of the base models. All the biomass trajectories calculated using these models fell within the confidence intervals for the base models and exhibited the same trends (Figures 35–42).

COMPARISON WITH OTHER TYPES OF MODELS

Several platforms are available for fitting SPMs. We compared the results for the base model fits obtained with JABBA with the output from SPiCT (Pedersen and Berg 2017) and CMSY++/BSM (Froese et al. 2017). The results showed that all the models produced similar parameter estimates. The trends in relative biomass and relative exploitation rates obtained with these models were also similar across the board, with only CMSY++ providing significantly different results, particularly for recent years. However, CMSY++ does not incorporate information on stock biomass and its results must be viewed with caution. For example, catches of schooling species may remain high despite an actual decline in biomass. In this type of situation, using data based solely on commercial catches may introduce bias in the results. Nevertheless, in general, the different sensitivity tests provided roughly the same results as the various configurations of the base models, showing the models' consistency and stability with respect to the basic assumptions.

SOURCES OF UNCERTAINTY

A surplus production model was used to describe the shrimp stocks trajectory over time. This model does not integrate information on the size or age structure of the population, and simplifies the productivity processes (recruitment, growth, natural mortality, etc.) to the estimated parameters *r* and *K*, which determine, respectively, the population growth rate and the support capacity of the environment. Essentially, next year's biomass is equal to this year's biomass, plus stock productivity, minus fishery catches.

Shrimp productivity has changed significantly over the past 30 years, with an initial increase in productivity that allowed the growth of the stock, followed by a significant decrease in productivity over the past decade that has greatly contributed to shrimp decline (Tamdrari et al. 2018). These changes are only partially captured by the model's process error. As a result, the SPM could be used heuristically to estimate the biomass that produces a maximum sustainable yield (MSY) from the fishery or B_{MSY}, and an exploitation rate at MSY or F_{MSY}. The B_{MSY} corresponds to a biomass at which the stock was productive, while the F_{MSY} corresponds to the approximate exploitation rate which prevailed when the stocks were at high abundance. The absolute annual values of biomass (B) and exploitation rate (F) estimated by the SPM do not make it possible to distinguish the effects of changes in productivity and fishing on stock dynamics, and are therefore considered unreliable and should not be overinterpreted. Only their trajectory over the entire series is informative, and the relationship between the relative biomass (B/B_{MSY}) and the relative exploitation rate (F/F_{MSY}) could serve as a guide to establish fishing removals which will reduce the risk of overfishing. The model is, however, not suitable for understanding future medium- and long-term responses of the stock to fishing on stock dynamics.

CONCLUSION

The results obtained show that the models had a good fit to the data and were able to reliably track the trajectories of stock biomass and exploitation rates. The results of the models were consistent with those of previous stock assessments: the Esquiman, Anticosti and Sept-Iles stocks have been declining for a number of years and, in 2022, reached the lowest biomass values observed since 1990, while the Estuary stock is currently fairly stable, with high values.

The estimation of a number of values such as maximum sustainable yield (MSY), the exploitation rate at MSY (F_{MSY}), the stock size (biomass) at MSY (B_{MSY}), and B_t/B_{MSY} and F_t/F_{MSY}, will be extremely useful in the review of the precautionary approach.

This model represents a positive step forward in the assessment of northern shrimp stocks in the ENGSL. However, as in all modelling, caution must be exercised when applying the model to ecosystem conditions outside the range of those already observed, and ongoing assessments of its effectiveness will be required.

ACKNOWLEDGEMENTS

We would like to thank Mathieu Boudreau for his initial analyses with the Bayesian surplus production model fit to the ENGSL northern shrimp stocks. We are also grateful to Jean-Martin Chamberland, Daniel Duplisea and Stéphane Plourde for reviewing this document.

REFERENCES CITED

Aeberhard, W.H., Mills Flemming, J., et Nielsen, A. 2018. Review of State-Space Models for Fisheries Science. Annu. Rev. Stat. Appl. 5(1): 215–235. doi:10.1146/annurev-statistics 031017-100427.

Bailey, J.A. 2012. *Bayesian Surplus Production modelling for American Plaice (Hippoglossoides platessoides)*. DFO Can. Sci. Advis. Sec. Res. Doc. 2012/036. ii + 144 p.

Bouch, P., Minto, C., et Reid, D.G. 2020. Comparative performance of data-poor CMSY and data-moderate SPiCT stock assessment methods when applied to data-rich, real-world stocks. ICES J. Mar. Sci. 78(1): 264–276.

Boudreau, M., et Duplisea, D. 2022. Outil d'aide à la décision pour la sélection des méthodes permettant d'obtenir des indicateurs de la santé et des points de référence pour des stocks limités en données. Rapp. manus. can. sci. halieut. aquat. 3237: vii + 67 pp.

Bourdages, H., Roux, M.-J., Marquis, M.C., Galbraith, P., and Isabel, L. 2022. Assessment of northern shrimp stocks in the Estuary and Gulf of St. Lawrence in 2021: commercial fishery and research survey data. DFO Can. Sci. Advis. Sec. Res. Doc. 2022/027. xiv + 195 p.

Bourdages, H., Bourret, A., and Parent, G.J. 2023. Delineation of stock assessment units for northern shrimp in the Estuary and northern Gulf of St. Lawrence. DFO Can. Sci. Advis. Sec. Res. Doc. 2023/082. vi + 30 p.

Caddy, J.F. 2004. Current usage of fisheries indicators and reference points, and their potential application to management of fisheries for marine invertebrates. Can. J. Fish. Aquat. Sci. 61(8): 1307-1324.

Carvalho, F., Winker, H., Courtney, D., Kapur, M., Kell, L., Cardinale, M., Schirripa, M., Kitakado, T., Yemane, D., Piner, K.R., Maunder, M.N., Taylor, I., Wetzel, C.R., Doering, K., Johnson, K.F., et Methot, R.D. 2021. A cookbook for using model diagnostics in integrated stock assessments. Fish. Res. 240: 105959.

Cousido-Rocha, M., Pennino, M.G., Izquierdo, F., Pax, A., Jojo, D., Tifoura, A., Zanni, M. Y., et Cervino, S. 2022. Surplus production models: a practical review of recent approaches. Rev. Fish Biol. Fish. 32, 1085–1102.

DFO. 2011. Reference points consistent with the precautionary approach for northern shrimp in the Estuary and Gulf of St. Lawrence. DFO Can. Sci. Advis. Sec. Sci. Advis. Rep. 2011/062.

DFO. 2022. Assessment of Northern Shrimp stocks in the Estuary and Gulf of St. Lawrence in 2021. DFO Can. Sci. Advis. Sec. Sci. Advis. Rep. 2022/006.

Froese, R., Demirel, N., Coro, G., Kleisner, K.M., et Winker, H. 2017. Estimating fisheries reference points from catch and resilience. Fish. 18(3), pp. 506-526.

Gelman, A., et Rubin, D.B. 1992. Inference from iterative simulation using multiple sequences. Statist. Sci. pp.457-472.

Graham, M. 1935. Modern theory of exploiting a fishery and application to North Sea trawling. Journal du Conseil Permanent International pour l'Exploration de la Mer, 10: 264–274.

Hvingel, C. 2015. The 2015 assessment of the North Sea / Skagerrak shrimp stock using a Bayesian surplus production model. NAFO SCR Doc. 15/59.

Hvingel, C. 2019. Shrimp (*Pandalus borealis*) in the Barents Sea – Stock assessment 2019. NAFO SCR Doc. 19/054.

Hvingel, C., et Kingsley, M.C.S. 2001. Assessment models for the West Greenland shrimp stock using a Bayesian approach. First results. NAFO SCR Doc.01/181. Serial No. N4570. 26 pp.

ICES. 2015. Report of the fifth Workshop on the Development of Quantitative Assessment Methodologies based on Life-history traits, exploitation characteristics, and other relevant parameters for data-limited stocks (WKLIFE V). ICES Expert Group reports (until 2018). Report.

Kruschke, J.K. 2021. Bayesian Analysis Reporting Guidelines. Nat. Hum. Behav. 5, pp.1282–1291.

Meyer, R., et Millar, R.B. 1999. BUGS in Bayesian stock assessments. Can. J. Fish. Aquat. Sci. 56, 1078–1086. .

Palomares, M.L.D., et Pauly, D (Editors). 2023. SeaLifeBase. World Wide Web electronic publication. version (04/2023).

Pauly, D., et Froese, R. 2021. MSY needs no epitaph—but it was abused, ICES J. Mar. Sci., 78(6), pp. 2204–2210.

Pedersen M. W., et Berg C. W. 2017. A stochastic surplus production model in continuous time. Fish. 18: 226–243.

Plummer, M. 2003. March. JAGS: A program for analysis of Bayesian graphical models using Gibbs sampling. In Proceedings of the 3rd international workshop on distributed statistical computing (Vol. 124, No. 125.10, pp. 1-10).

Pons, M., Cope, J.M., et Kell, L.T. 2020. Comparing performance of catch-based and length based stock assessment methods in data-limited fisheries. Can. J. Fish. Aquat. Sci. 77(6): 1026–1037. doi:10.1139/cjfas-2019-0276.

Punt, A.E. 2023. Those who fail to learn from history are condemned to repeat it: A perspective on current stock assessment good practices and the consequences of not following them. Fish. Res. 261: 106642.

Punt, A.E., et Hilborn, R. 1997. Fisheries stock assessment and decision analysis: The Bayesian approach. Rev. Fish Biol. Fish.,7, pp. 35–63.

Punt, A.E., Smith, A.D.M., Smith, D.C., Tuck, G.N., et Klaer, N.L. 2014. Selecting relative abundance proxies for BMSY and BMEY. ICES J. Mar. Sci. 71(3): 469–483. doi:10.1093/icesjms/fst162.

Schaefer, M.B. 1954. Some Aspects of the Dynamics of Populations Important to the Management of the Commercial Marine Fisheries. Inter-American Tropical Tuna Comm. Bull. 1(2).

Su, Y.-S., et Yajima, M. 2012. R2jags: A Package for Running jags from R.

Tamdrari, H., Benoît, H.P., Hanson J.M., Bourdages, H., and Brêthes, J.-C. 2018. Habitat associations and assemblage structure of shrimp species in the Gulf of St. Lawrence (Canada) following dramatic increases in abundance. Mar. Ecol. Prog. Ser. 596: 95-112.

Thorson, J.T., Cope, J.M., Branch, T.A., Jensen, O.P., et Walters, C.J. 2012. Spawning biomass reference points for exploited marine fishes, incorporating taxonomic and body size information. Can. J. Fish. Aquat. Sci. 69, 1556–1568.

Thorson, J.T., Ono, K., et Munch, S.B. 2014. A Bayesian approach to identifying and compensating for model misspecification in population models. Ecology 95(2): 329-341.

Vehtari, K., Gelman, A., Simpson, D., Carpenter, B., et Bürkner, P.C. 2021. Rank-normalization, folding, and localization: An improved R-hat for assessing convergence of MCMC (with discussion). Bayesian Data Anal. 16(2), 667-–718. doi:10.1214/20-BA1221

Verhulst, P.-F. 1838. Notice sur la loi que la population suit dans son accroissement. Correspondance Mathématique et Physique, 10: 113–121.

Winker, H., Carvalho, F., et Kapur, M. 2018. JABBA: just another Bayesian biomass assessment. Fish. Res. 204, pp. 275-288.

Winker, H., Carvalho, F., Thorson, J.T., Kell, L.T., Parker, D., Kapur, M., Sharma, R., Booth, A.J., et Kerwath, S.E. 2020. JABBA-Select: Incorporating life history and fisheries' selectivity into surplus production models. Fish. Res. 222, p.105355.

Zhou, S., Punt, A.E., Deng, R., Dichmont, C.M., Ye, Y., et Bishop, J. 2009. Modified hierarchical Bayesian biomass dynamics models for assessment of short-lived invertebrates: A comparison for tropical tiger prawns. Mar. Freshw. Res. 60: 1298–1308.

TABLES

Table 1. Time series of landings (t) in stock area from 1982 to 2022.

Year	Esquiman	Anticosti	Sept-Iles	Estuary
1982	2,111	2,402	3,836	152
1983	2,242	2,861	3,711	158
1984	1,578	1,276	4,443	248
1985	1,421	2,767	4,418	164
1986	1,592	3,314	4,242	262
1987	2,685	3,403	5,430	523
1988	4,335	2,844	6,047	551
1989	4,614	4,226	6,281	629
1990	3,303	4,723	6,839	507
1991	4,773	4,554	6,447	505
1992	3,149	4,146	4,973	489
1993	4,683	4,622	5,654	496
1994	4,689	3,823	7,196	502
1995	4,800	2,171	9,177	486
1996	5,123	1,177	11,306	505
1997	5,957	3,244	10,551	549
1998	6,554	5,910	10,003	634
1999	6,732	3,774	12,487	646
2000	7,396	4,197	13,904	739
2001	7,815	3,655	12,709	832
2002	8,250	4,023	16,108	799
2003	6,773	3,454	16,645	796
2004	8,593	5,571	20,790	1,033
2005	8,867	3,176	17,664	1,001
2006	8,957	5,053	19,013	1,029
2007	9,208	9,361	16,464	1,022
2008	9,110	9,282	16,325	1,017
2009	9,473	9,443	16,074	993
2010	9,541	10,087	15,768	906
2011	9,177	9,561	14,646	880
2012	10,244	8,187	12,596	956
2013	9,149	7,672	14,227	1,117
2014	8,408	8,714	12,440	984
2015	8,220	9,161	12,425	1,075
2016	7,081	8,680	12,141	1,027
2017	7,024	6,928	6,946	899
2018	5,971	6,285	4,189	214
2019	5,981	6,848	4,012	199
2020	5,992	6,182	5,101	570
2021	5,535	6,233	4,982	579
2022	4,253	3,717	3,909	497

Table 2. Time series of total biomass index values (t) in stock from 1982 to 2022.

Year	Esquiman	Anticosti	Sept-Iles	Estuary
1990	20,358	36,229	31,866	2,011
1991	15,336	21,973	43,033	2,219
1992	9,490	23,782	18,642	1,803
1993	9,116	14,968	25,037	1,486
1994	11,988	11,767	33,251	2,088
1995	21,198	29,739	42,200	344
1996	20,525	57,830	56,354	2,862
1997	46,764	35,790	63,502	1,764
1998	27,492	27,857	72,819	727
1999	33,550	31,484	66,381	3,015
2000	31,272	43,272	97,138	3,371
2001	29,755	30,139	80,285	1,858
2002	13,395	53,610	86,963	1,526
2003	60,250	76,913	194,703	3,343
2004	38,719	57,708	122,516	2,893
2005	46,872	70,211	99,464	2,385
2006	50,305	42,620	82,758	1,947
2007	31,708	72,918	111,320	3,482
2008	29,685	28,870	97,972	10,715*
2009	35,140	46,271	77,580	9,991*
2010	32,947	38,440	79,291	7,898*
2011	47,211	21,827	53,408	7,266*
2012	31,079	28,530	72,082	7,993*
2013	35,399	28,898	57,704	6,764*
2014	31,002	33,574	84,410	10,940*
2015	22,056	34,597	69,072	5,381*
2016	25,432	20,748	44,581	7,486*
2017	18,996	26,624	21,684	2,420*
2018	17,478	19,170	14,971	6,924*
2019	23,251	18,905	20,941	9,742*
2020	11,470	20,947	27,458	2,315*
2021	14,404	15,383	11,966	12,949*
2022	11,619	8,924	41,43	25,504*

*: Beginning in 2008, sampling was expanded by adding strata in the shallow portion (37–183 m) of the Estuary.

Table 3. Prior distributions used in the base model for each stock.

	Esquiman	Anticosti	Sept-Iles	Estuary
r mean	0.58	0.58	0.58	0.58
r log SD	0.53	0.53	0.53	0.53
K low	35,323	34,781	71,689	3,852
K high	211,936	208,689	430,135	23,114
B_1/K mean	0.2	0.2	0.2	0.5
B_1/K CV	0.25	0.25	0.25	0.25
σ_η^2 (igamma)	(0.001, 0.001)	(0.001, 0.001)	(0.001, 0.001)	(0.001, 0.001)
σ_{fix}^2(fixed.obsE)	0.2	0.2	0.2	0.2
$\sigma_{est,t}^2$ (sigma.est)	(0.001, 0.001)	(0.001, 0.001)	(0.001, 0.001)	(0.001, 0.001)
Catches CV	0.1	0.1	0.1	0.1

Table 4. Diagnostic statistics for model convergence and goodness of fit for the four stocks. R-hat designates the potential scale reduction statistic; ESS, effective sample size; DIC, deviation information criterion; RMSE, root mean square error; and SDNR, standard deviation of the normalized residuals.

Statistic	Anticosti	Esquiman	Estuary	Sept-Iles
R-hat (Vehtari et al. 2021) < 1.1	TRUE	TRUE	TRUE	TRUE
R-hat (Gelman and Rubin 1992) < 1.1	TRUE	TRUE	TRUE	TRUE
min ess	120	66	38	220
max ess	15,000	15,000	15,000	15,000
mean ess	4,265	4,410	3,032	4,684
min bulk ess	140.1	63.83	85.77	206.9
max bulk ess	15,329.5	15,077.63	15,181.57	14,963.7
mean bulk ess	2,900.6	3,194.84	3,198.44	4,329.3
min tail ess	195.8	167.4	135	227.3
max tail ess	14,823.4	15,042.7	15,201.4	14,904.9
mean tail ess	3,690	4,215.9	4,601.6	5,525
DIC	445.6	441.5	166.7	478.2
RMSE	31.3	29.4	70.4	23.1
SDNR	0.93	0.9	0.97	0.9

Table 5. Posterior distributions of the base model parameters for the Esquiman stock.

Parameter	Median	CI low	CI high
K	82,912.363	47,518.345	166,498.828
r	0.416	0.219	0.704
B_1/K	0.199	0.129	0.302
F_{MSY}	0.208	0.109	0.352
B_{MSY}	41,456.181	23,759.173	83,249.414
MSY	8,525.147	6,237.247	12,482.450
B_{2022}/B_{MSY}	0.414	0.183	0.942
F_{2022}/F_{MSY}	1.245	0.436	2.533
q	0.823	0.326	1.583
σ_{η}^2	0.022	0.001	0.043
$\sigma_{\varepsilon,t}^2$	0.050	0.005	0.147

Table 6. Posterior distributions of the base model parameters for the Anticosti stock.

Parameter	Median	CI low	CI high.
K	73,783.932	46,212.731	140,920.957
r	0.372	0.207	0.618
B_1/K	0.249	0.171	0.332
F_{MSY}	0.186	0.104	0.309
B_{MSY}	36,891.966	23,106.365	70,460.479
MSY	6,877.157	5,606.349	9,339.246
B_{2022}/B_{MSY}	0.284	0.130	0.555
F_{2022}/F_{MSY}	1.894	0.929	3.930
q	1.080	0.673	1.618
σ_{η}^2	0.007	0.001	0.039
$\sigma_{\varepsilon,t}^2$	0.054	0.005	0.135

Table 7. Posterior distributions of the base model parameters for the Sept-Iles stock.

Parameter	Median	CI low	CI high
K	112,016.900	66,223.050	216,946.900
r	0.516	0.247	0.963
B_1/K	0.158	0.102	0.242
F_{MSY}	0.258	0.124	0.482
B_{MSY}	56,008.460	33,111.530	108,473.400
MSY	14,599.800	10,007.580	19,641.610
B_{2022}/B_{MSY}	0.048	0.039	0.091
F_{2022}/F_{MSY}	5.383	3.213	7.800
q	2.025	1.063	3.646
σ_{η}^2	0.032	0.004	0.044
$\sigma_{\varepsilon,t}^2$	0.014	0.001	0.079

Table 8. Posterior distributions of the base model parameters for the Estuary stock.

Parameter	Median	CI low	CI high
K	8,669.311	4,611.354	17,036.034
r	0.502	0.252	1.165
B_1/K	0.524	0.294	0.749
F_{MSY}	0.251	0.126	0.583
B_{MSY}	4,334.655	2,305.677	8,518.017
MSY	1,023.111	719.336	2,776.025
B_{2022}/B_{MSY}	1.383	0.640	2.204
F_{2022}/F_{MSY}	0.361	0.091	0.878
q	1.862	0.631	4.358
σ_{η}^2	0.008	0.001	0.040
$\sigma_{\varepsilon,t}^2$	0.282	0.112	0.740

Table 9. Prior distributions of parameters used in the different sensitivity tests. Parameters differing from those in the base models are shown in bold.

ID	Scenario	r	r log SD	K	K log standard deviation	B_{MSY}/K	B_1/K	Years
base	base	0.58	0.5	(2–12x_max_catch)/r	0.45	0.5	0.2	1990–2022
s1	r_low	**0.30**	0.5	(2–12x_max_catch)/r	0.45	0.5	0.2	1990–2022
s2	r_high	**0.90**	0.5	(2–12x_max_catch)/r	0.45	0.5	0.2	1990–2022
s3	r_sd_low	0.58	**0.1**	(2–12x_max_catch)/r	0.45	0.5	0.2	1990–2022
s4	r_sd_high	0.58	**1.0**	(2–12x_max_catch)/r	0.45	0.5	0.2	1990–2022
s5	K_low	0.58	0.5	**(2–6x_max_catch)/r**	0.45	0.5	0.2	1990–2022
s6	K_high	0.58	0.5	**(8–12x_max_catch)/r**	0.45	0.5	0.2	1990–2022
s7	K_sd_high	0.58	0.5	**(2–24x_max_catch)/r**	**0.83**	0.5	0.2	1990–2022
s8	B_{MSY}/K = 0.4	0.58	0.5	(2–12x_max_catch)/r	0.45	**0.4**	0.2	1990–2022
s9	B_1/K = 0.5	0.58	0.5	(2–12x_max_catch)/r	0.45	0.5	**0.5**	1990–2022
s10	B_1/K =0.7	0.58	0.5	(2–12x_max_catch)/r	0.45	0.5	**0.7**	1990–2022
s11	82–22	0.58	0.5	(2–12x_max_catch)/r	0.45	0.5	0.2	**1982–2022**
s12	90–05	0.58	0.5	(2–12x_max_catch)/r	0.45	0.5	0.2	**1990–2005**
s13	05–22	0.58	0.5	(2–12x_max_catch)/r	0.45	0.5	0.2	**2005–2022**

FIGURES

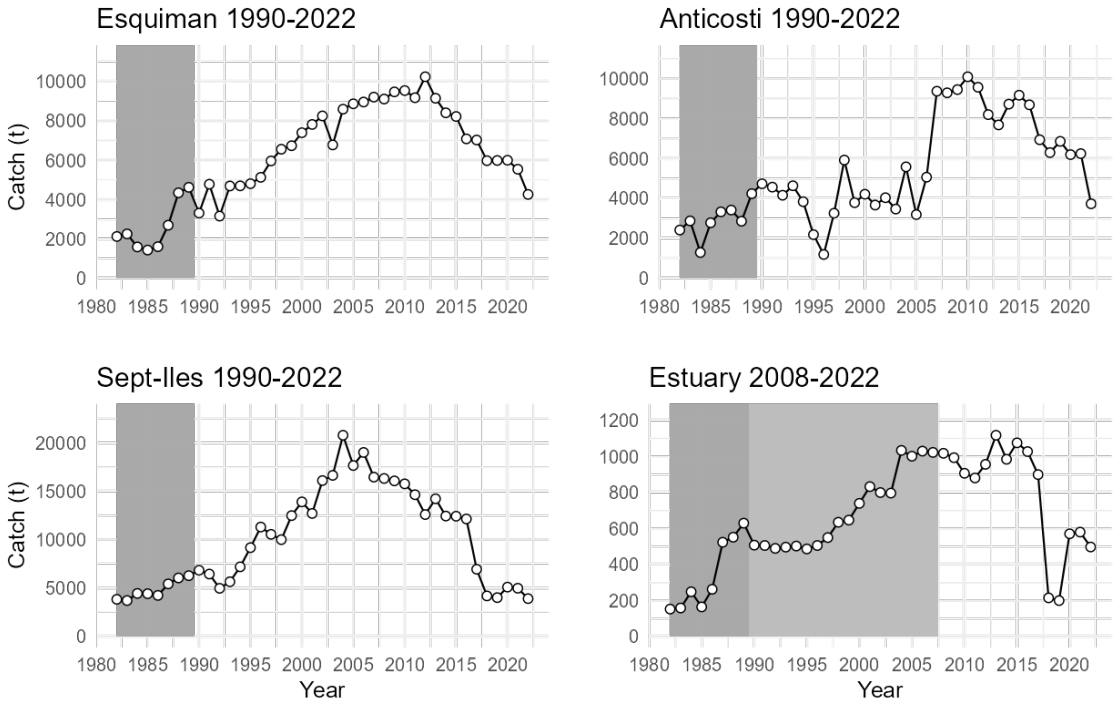

Figure 1. Annual landings (catches) in tonnes in the four stocks. The dark grey background indicates the years not used in the base model. The light grey background in the graph for the Estuary indicates the years before additional strata were sampled in the bottom trawl survey.

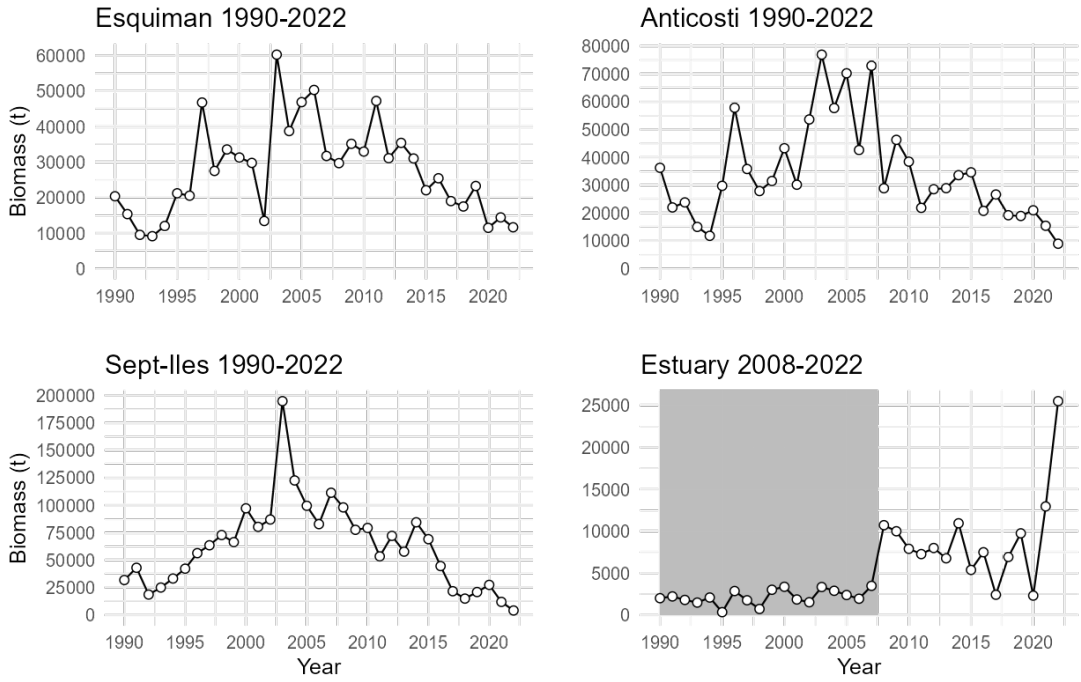

Figure 2. Total annual biomass in tonnes in the four stocks. The dark grey background indicates the years not used in the base model.

Esquiman

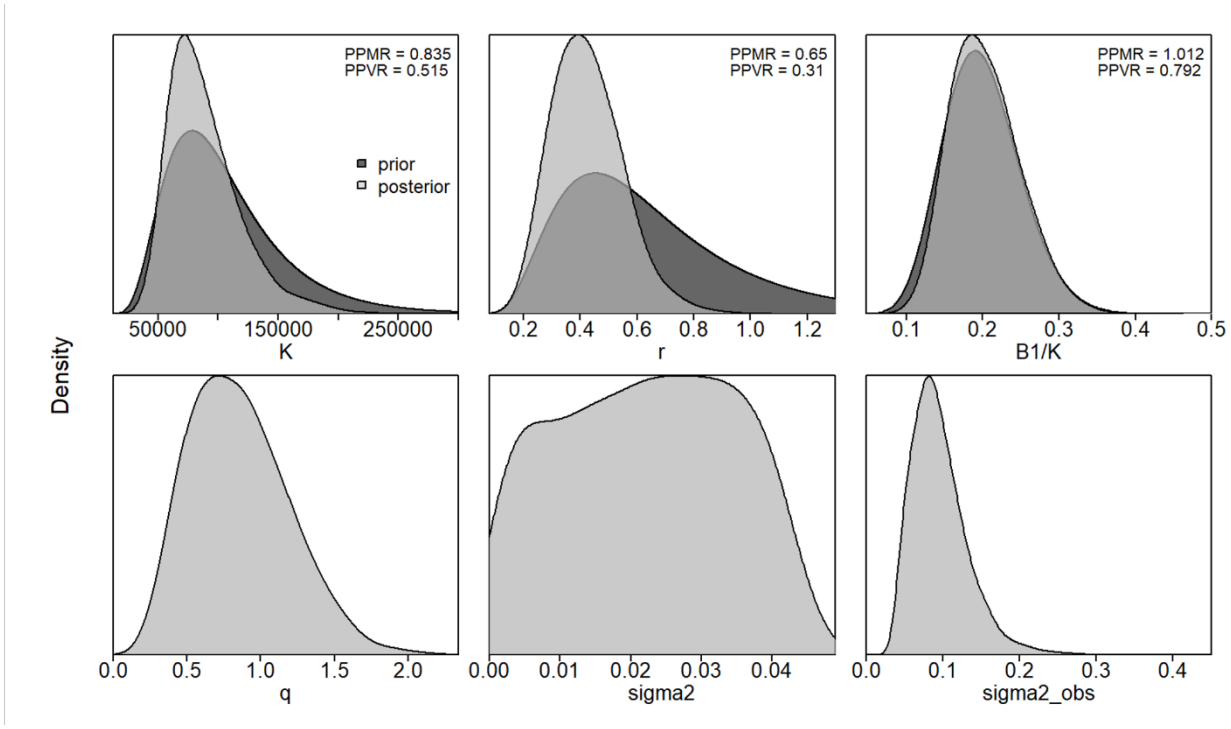

Figure 3. Prior distributions (dark grey) and posterior distributions (light grey) of the parameters used in the base model for Esquiman. The parameters examined include carrying capacity (K), intrinsic rate of increase (r), biomass as a proportion of carrying capacity in the first year of the time series (B_1/K), the biomass index catchability coefficient (q), the process error variance σ_η^2 (sigma2) and the observation error variance $\sigma_{\varepsilon,t}^2$ (sigma2_obs). Posterior distributions were plotted using generic kernel densities.

Esquiman

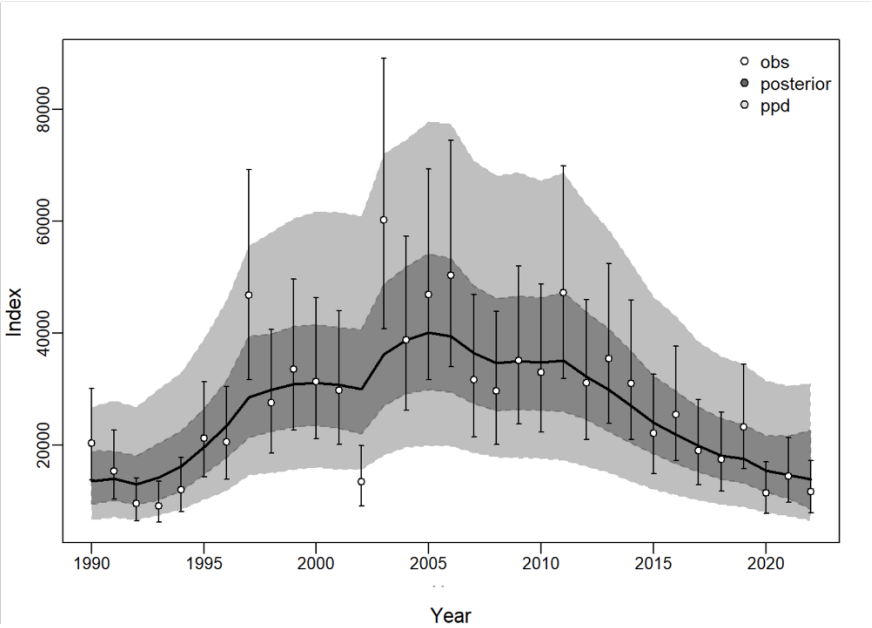

Figure 4. Total biomass index values observed for the Esquiman stock (white dots and associated error bars) and the trajectory estimated by the base model (black line). The shaded areas represent the posterior distribution of the predicted values (dark grey) and the predictive posterior distribution (PPD) (light grey).

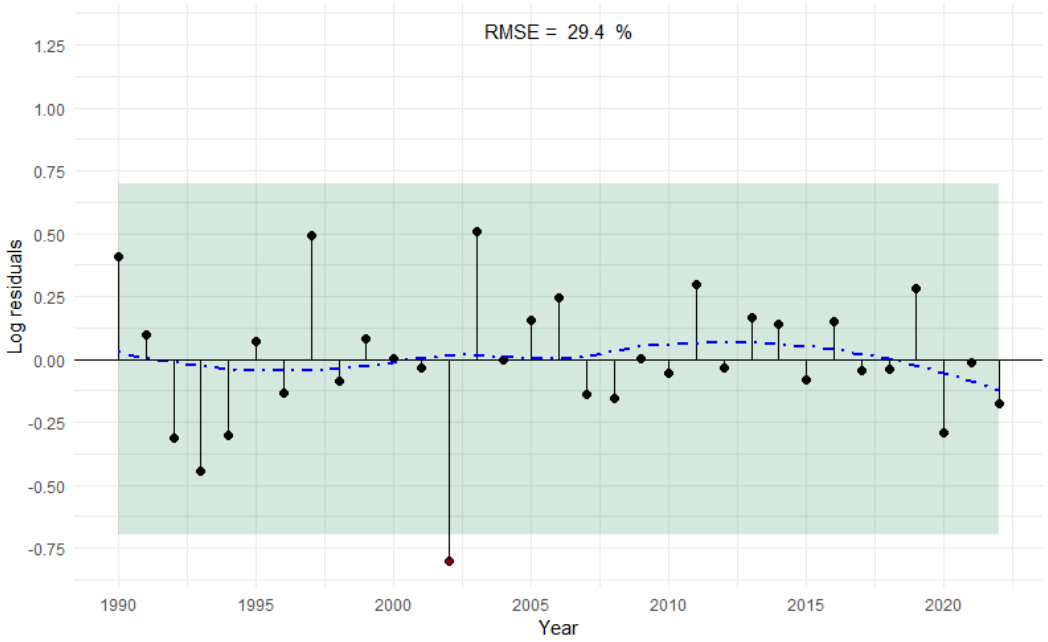

Figure 5. Residual diagnostics for the base model for the Esquiman stock, plotted on a log scale of biomass index values. The dot-dash blue line represents the LOESS-smoothed residuals, while the green background represents the results of the Wald-Wolfowitz test. The RMSE corresponds to the mean absolute error in percentage terms.

Esquiman

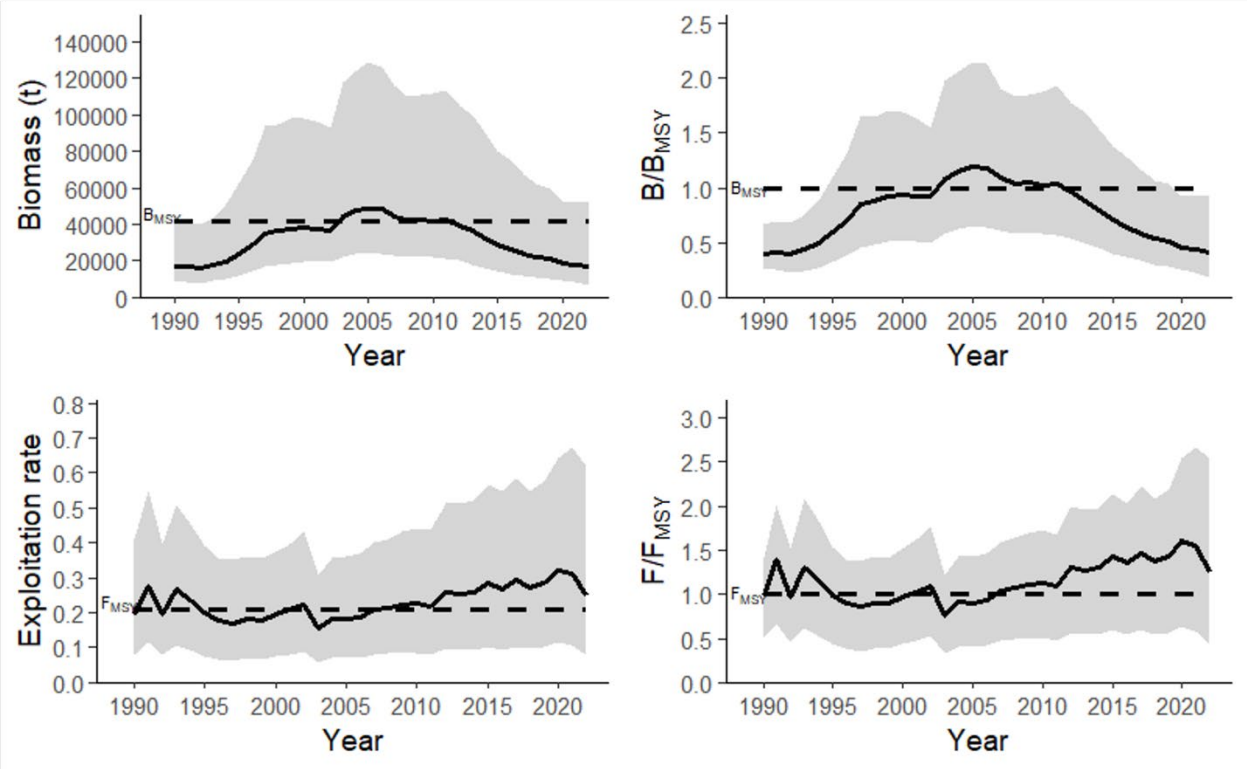

Figure 6. Estimated trajectories for Esquiman stock biomass (B_t) and fishing mortality (F_t), scaled to the maximum sustainable yield (B/B_{MSY} and F/F_{MSY}). The shaded area represents the 95% confidence interval.

Esquiman

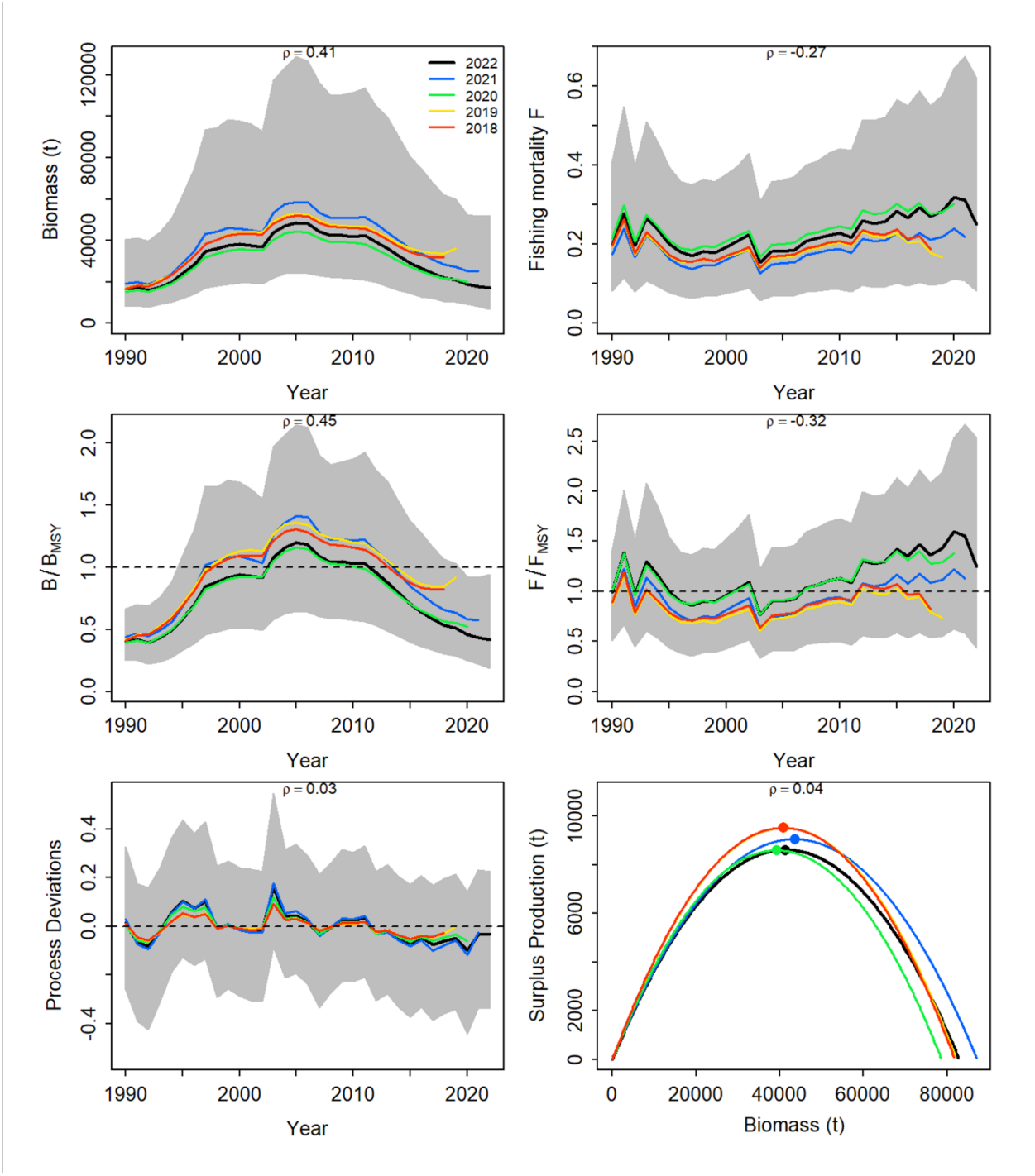

Figure 7. Retrospective analysis for the Esquiman stock (2018–2022). The mean Mohn's rho values are shown on each graph.

Esquiman

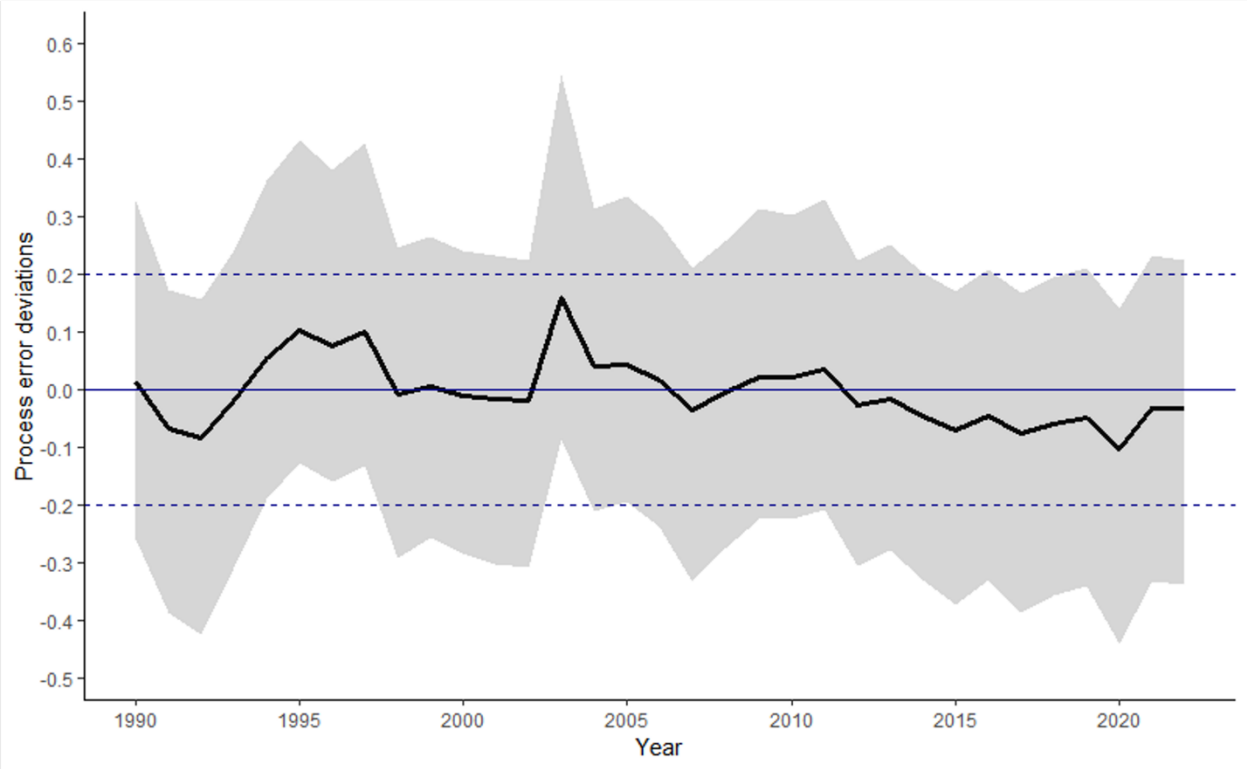

Figure 8. Process error deviation in the Esquiman model. The black line represents the median value of the posterior distribution, while the 95% CI is shown in grey. The solid blue line represents the trend for biomass generated by the deterministic portion of the model, while the dashed blue lines are provided to make the graph easier to read.

Esquiman

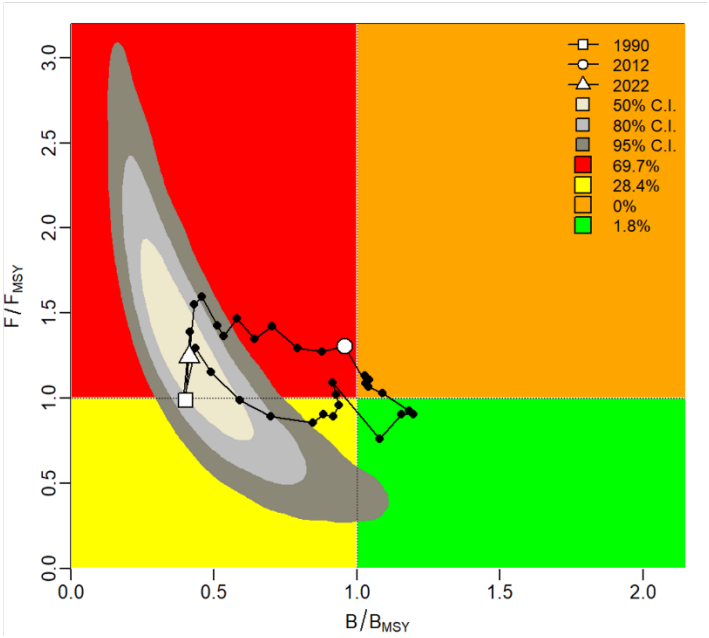

Figure 9. Kobe-type plot for the base case scenario for the Esquiman stock. The black line shows the estimated trajectory (1990–2022) between F/F_{MSY} and B/B_{MSY}. The grey shaded areas show the confidence intervals for the terminal year (50%, 80% and 95%). The probabilities of the terminal year being located in one of the quadrants are indicated in the legend.

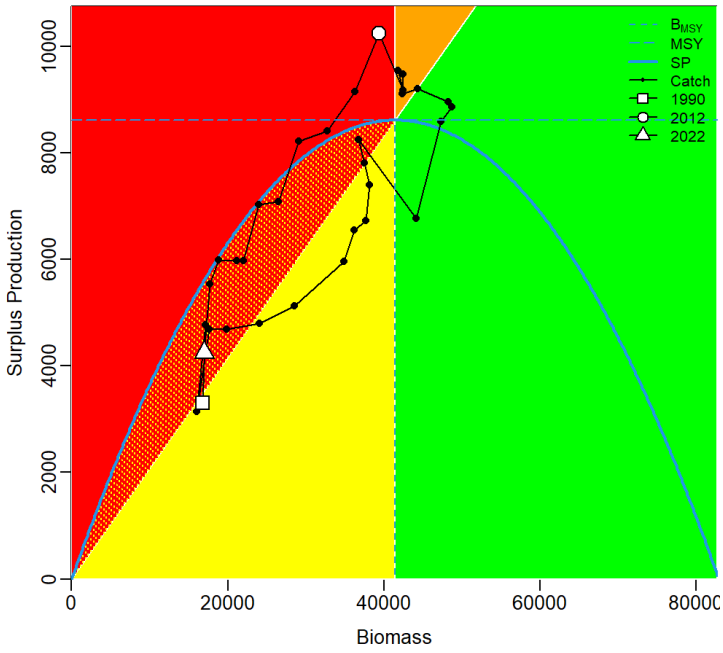

Figure 10. SP-phase-type plot showing the estimated surplus production curve (blue line) and the catch trajectory (black line) as a function of biomass for the base case scenario for the Esquiman stock. The blue dashed lines show the estimated values for maximum sustainable yield.

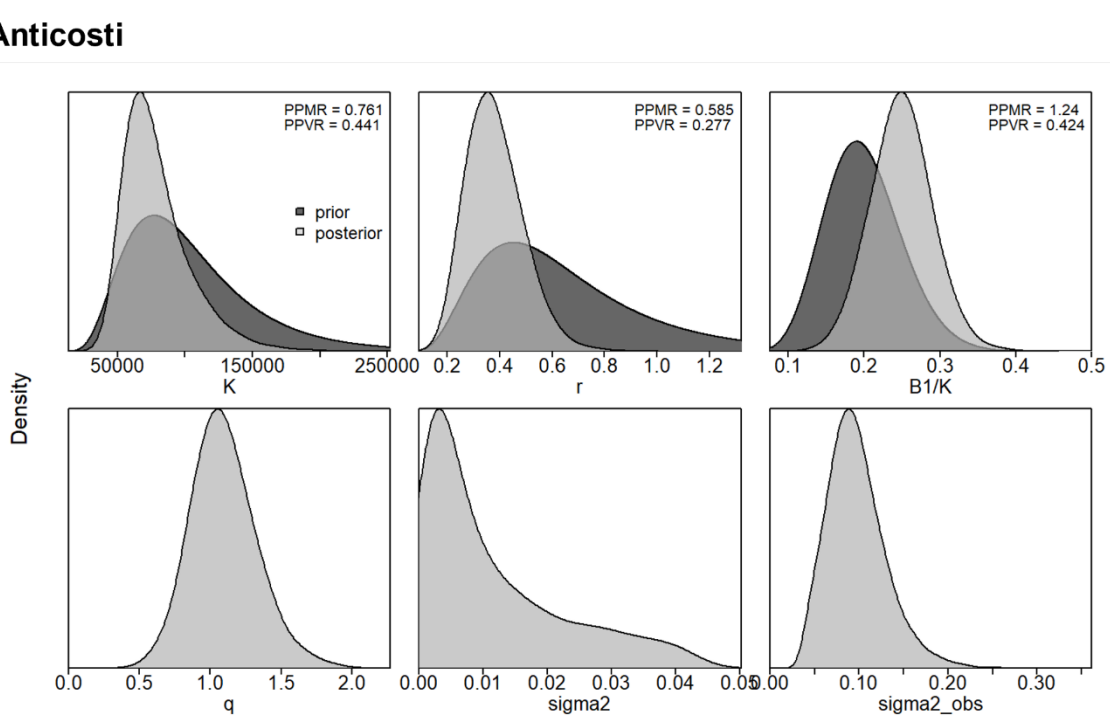

Figure 11. Prior distributions (dark grey) and posterior distributions (light grey) of the parameters used in the base model for Anticosti. The parameters examined include carrying capacity (K), intrinsic rate of increase (r), biomass as a proportion of carrying capacity in the first year of the time series (B_1/K), the biomass index catchability coefficient (q), the process error variance σ_{η}^2 (sigma2) and the observation error variance $\sigma_{\varepsilon,t}^2$ (sigma2_obs). Posterior distributions were plotted using generic kernel densities.

Anticosti

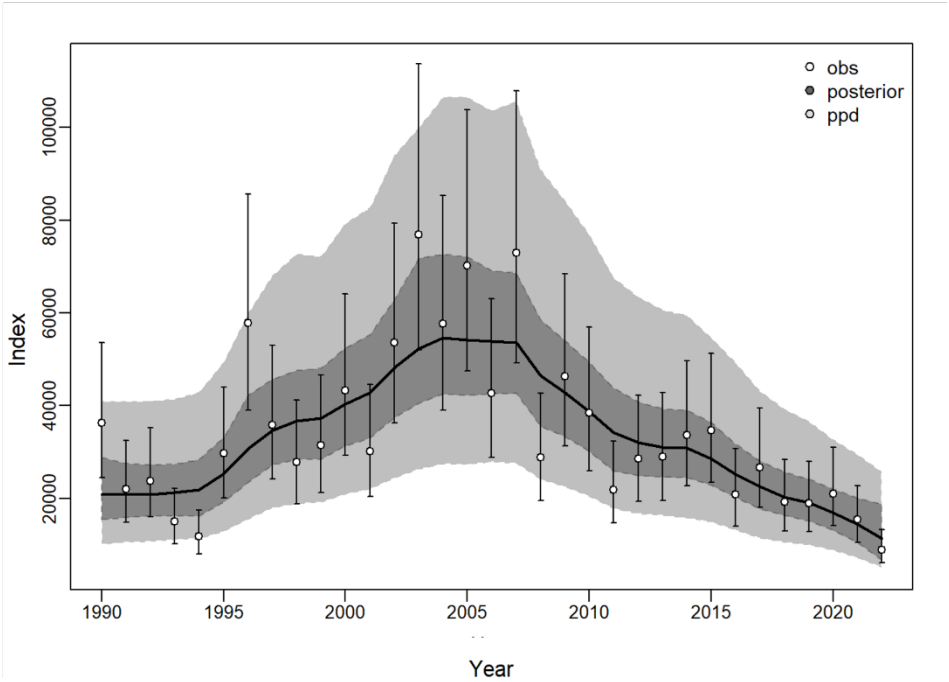

Figure 12. Total biomass index values observed for the Anticosti stock (white dots and associated error bars) and the trajectory estimated by the base model (black line). The shaded areas represent the posterior distribution of the predicted values (dark grey) and the predictive posterior distribution (PPD) (light grey).

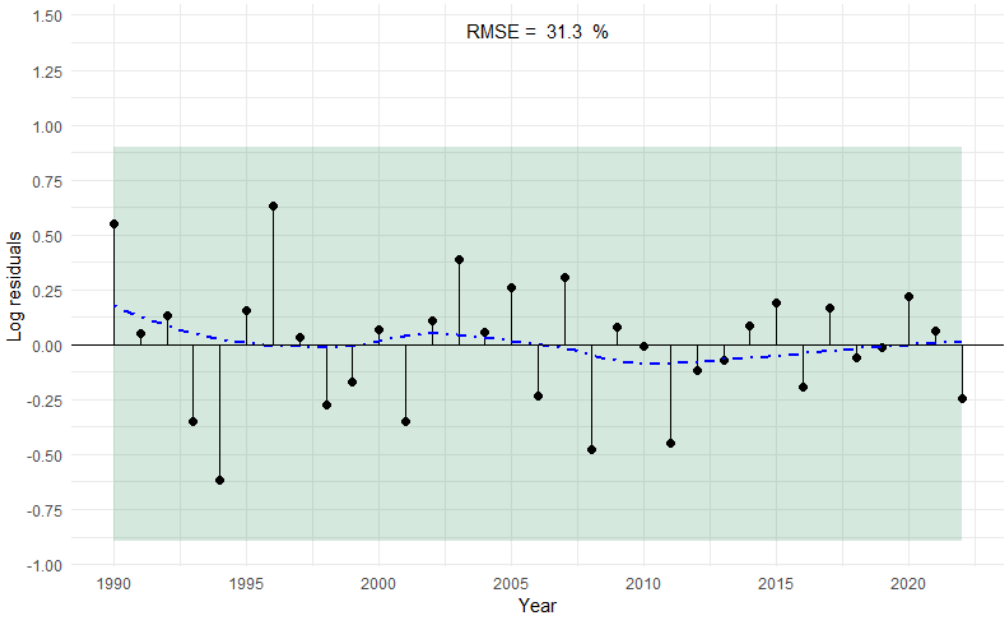

Figure 13. Residual diagnostics for the base model for the Anticosti stock, plotted on a log scale of biomass index values. The dot-dash blue line represents the LOESS-smoothed residuals, while the green background represents the results of the Wald-Wolfowitz test. The RMSE corresponds to the mean absolute error in percentage terms.

Anticosti

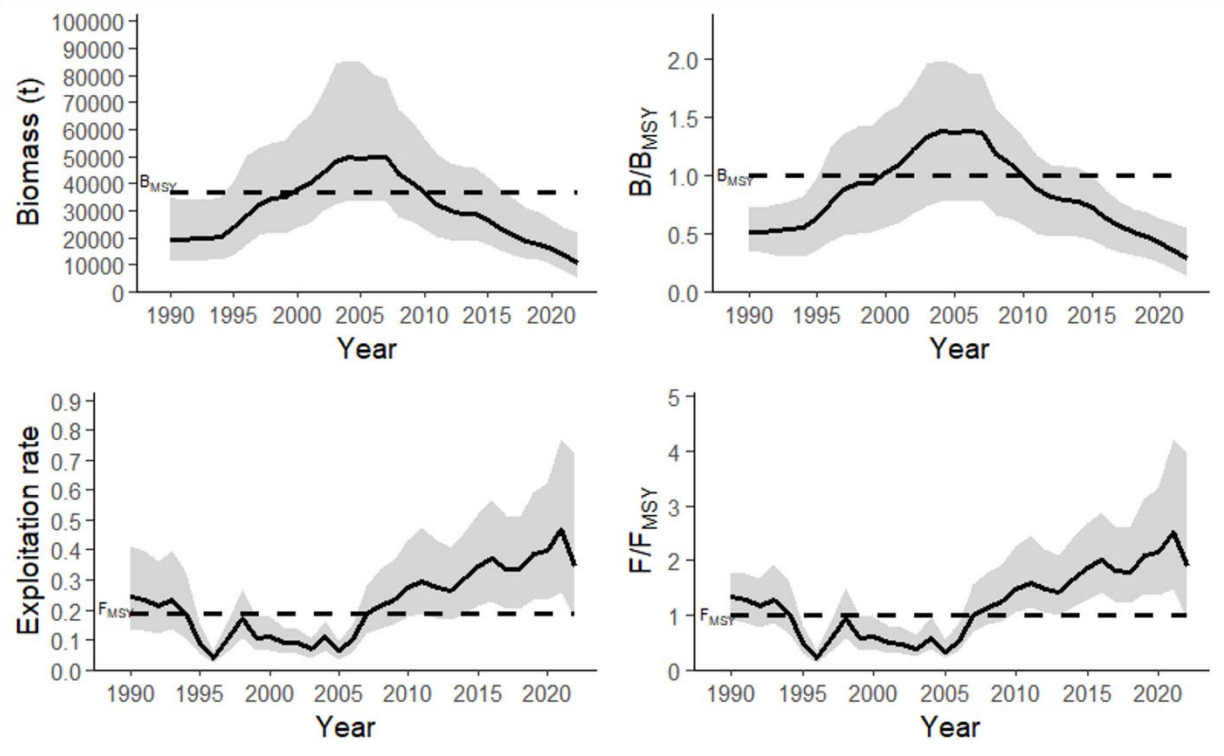

Figure 14. Estimated trajectories for Anticosti stock biomass (B_t) and fishing mortality (F_t), scaled according to the maximum sustainable yield (B/B_{MSY} and F/F_{MSY}). The shaded area represents the 95% confidence interval.

Anticosti

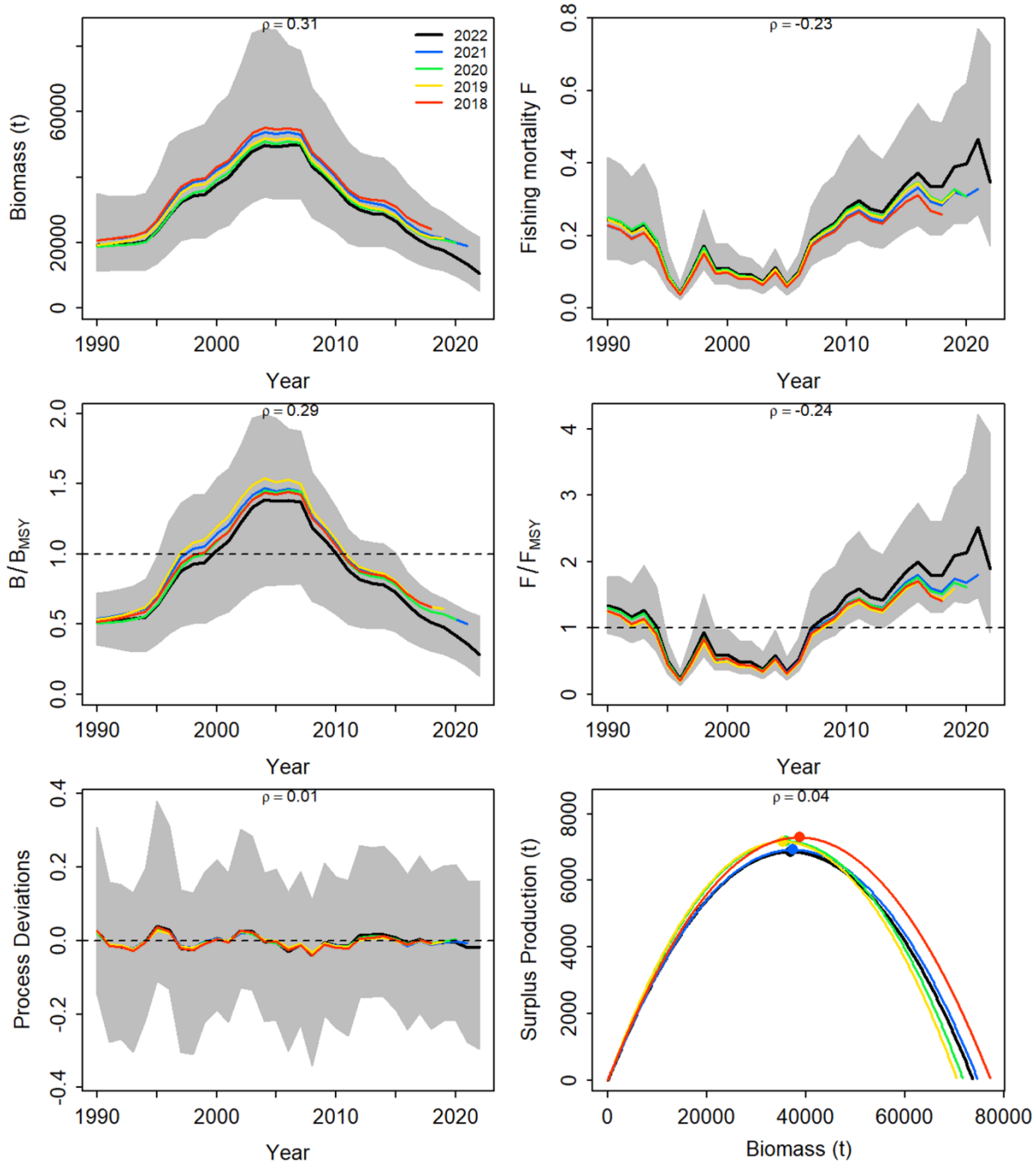

Figure 15. Retrospective analysis for the Anticosti stock (2018–2022). The mean Mohn's rho values are shown on each graph.

Anticosti

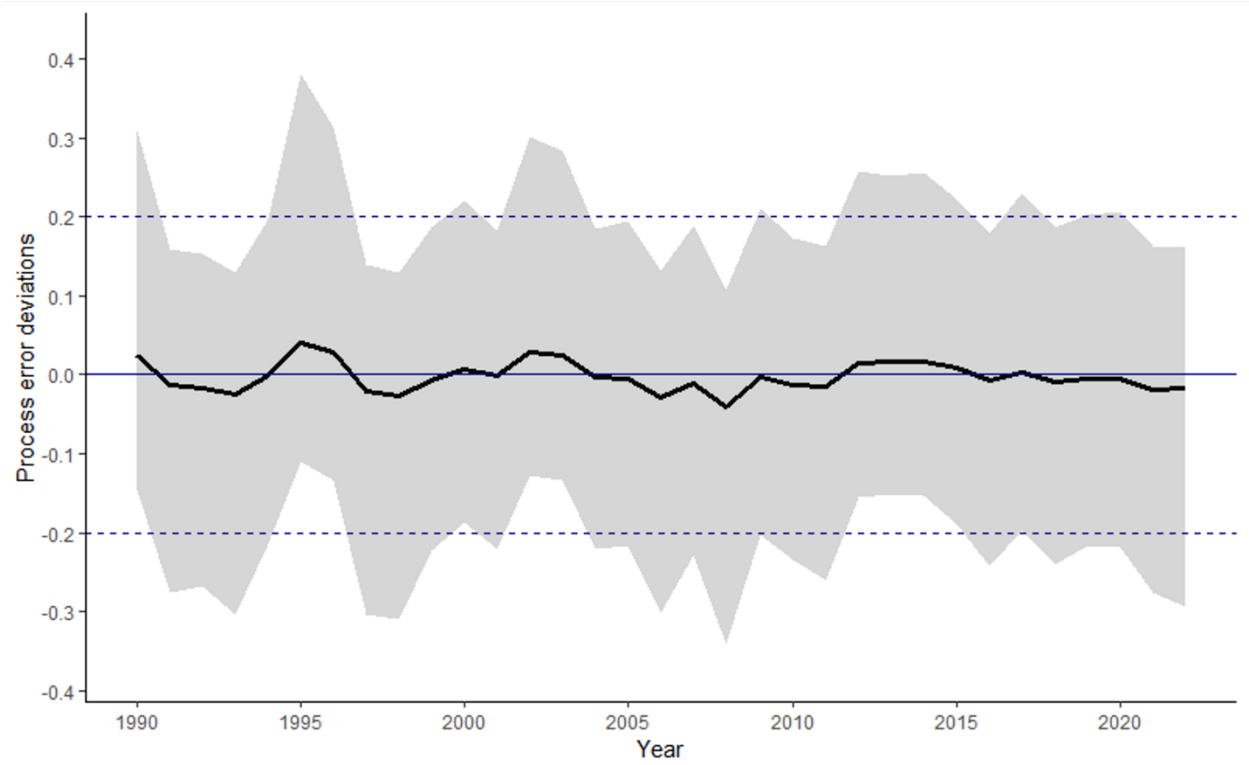

Figure 16. Process error deviation in the Anticosti model. The black line represents the median value of the posterior distribution, while the 95% CI is shown in grey. The solid blue line represents the trend for biomass generated by the deterministic portion of the model, while the dashed blue lines are provided to make the graph easier to read.

Anticosti

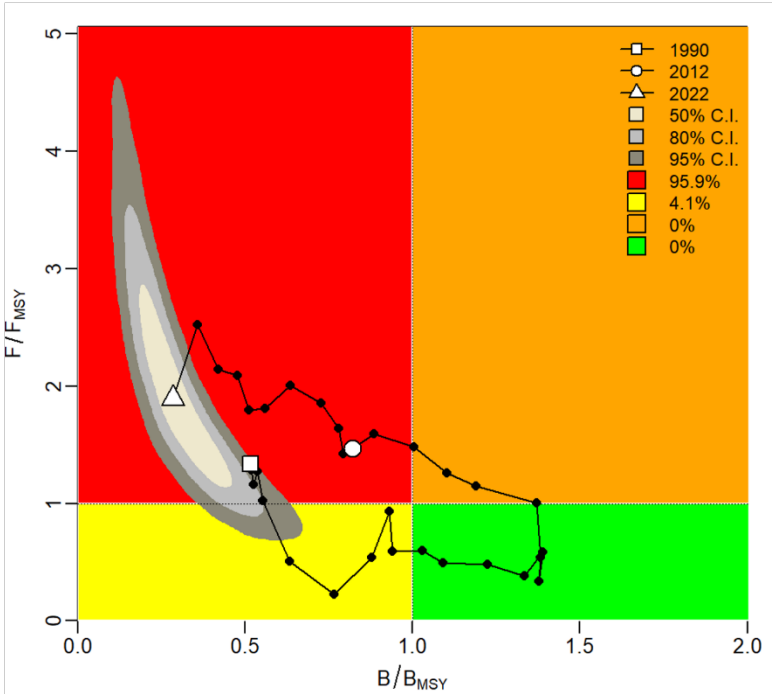

Figure 17. Kobe-type plot for the base case scenario for the Anticosti stock. The black line shows the estimated trajectory (1990–2022) between F/F_{MSY} and B/B_{MSY}. The grey shaded areas show the confidence intervals for the terminal year (50%, 80% and 95%). The probabilities of the terminal year being located in one of the quadrants are indicated in the legend.

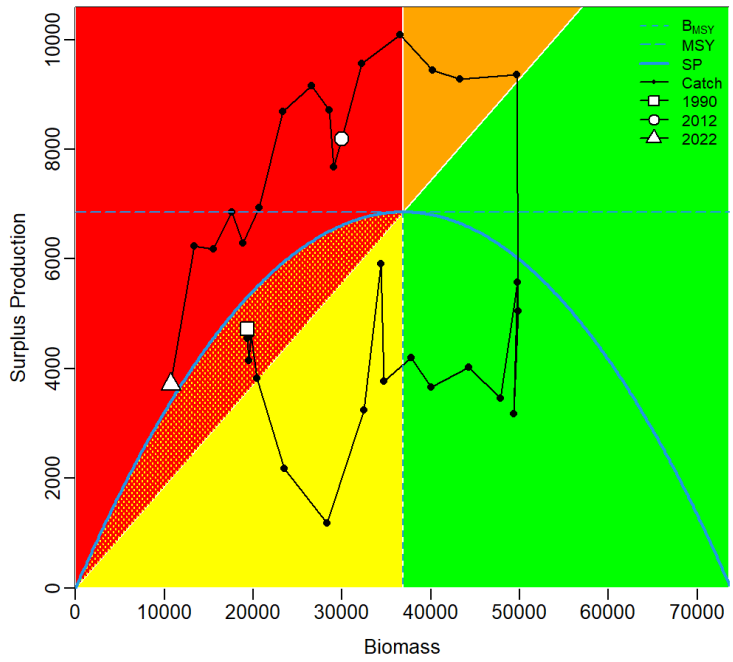

Figure 18. SP-phase-type plot showing the estimated surplus production curve (blue line) and the catch trajectory (black line) as a function of biomass for the base case scenario for the Anticosti stock. The blue dashed lines show the estimated values for maximum sustainable yield.

Sept-Iles

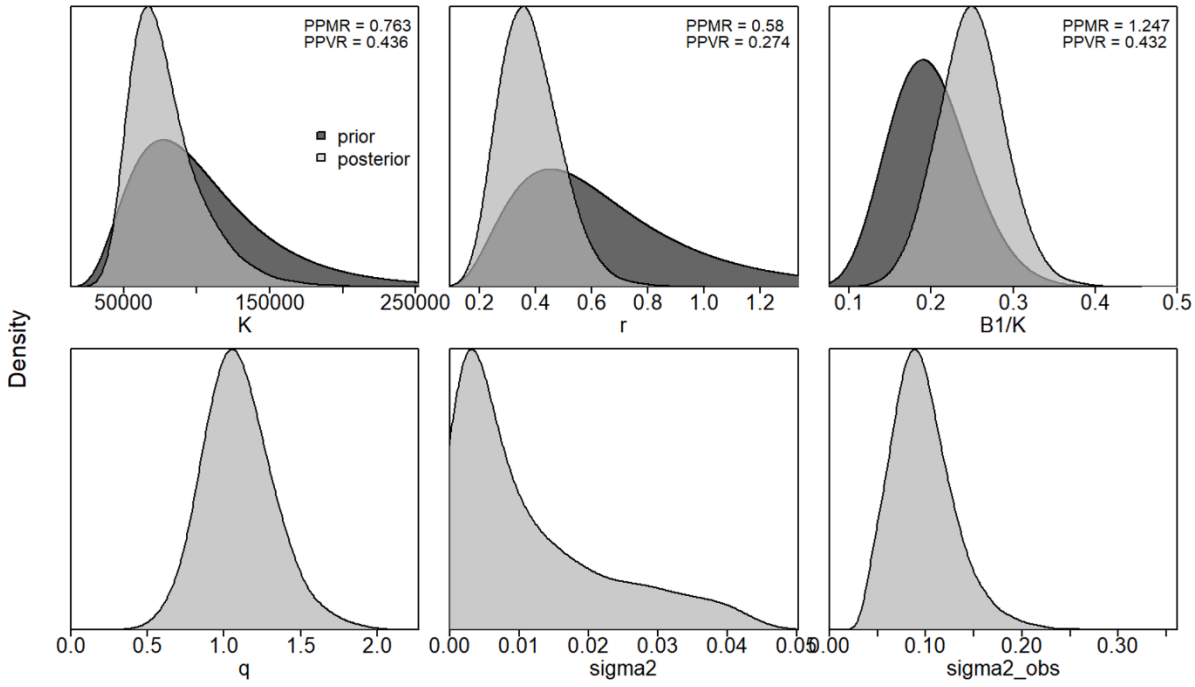

Figure 19. Prior distributions (dark grey) and posterior distributions (light grey) of the parameters used in the base model for Sept-Iles. The parameters examined include carrying capacity (K), intrinsic rate of increase (r), biomass as a proportion of carrying capacity in the first year of the time series (B_1/K), the biomass index catchability coefficient (q), the process error variance σ^2_{η} (sigma2) and the observation error variance $\sigma^2_{\varepsilon,t}$ (sigma2_obs). Posterior distributions were plotted using generic kernel densities.

Sept-Îles

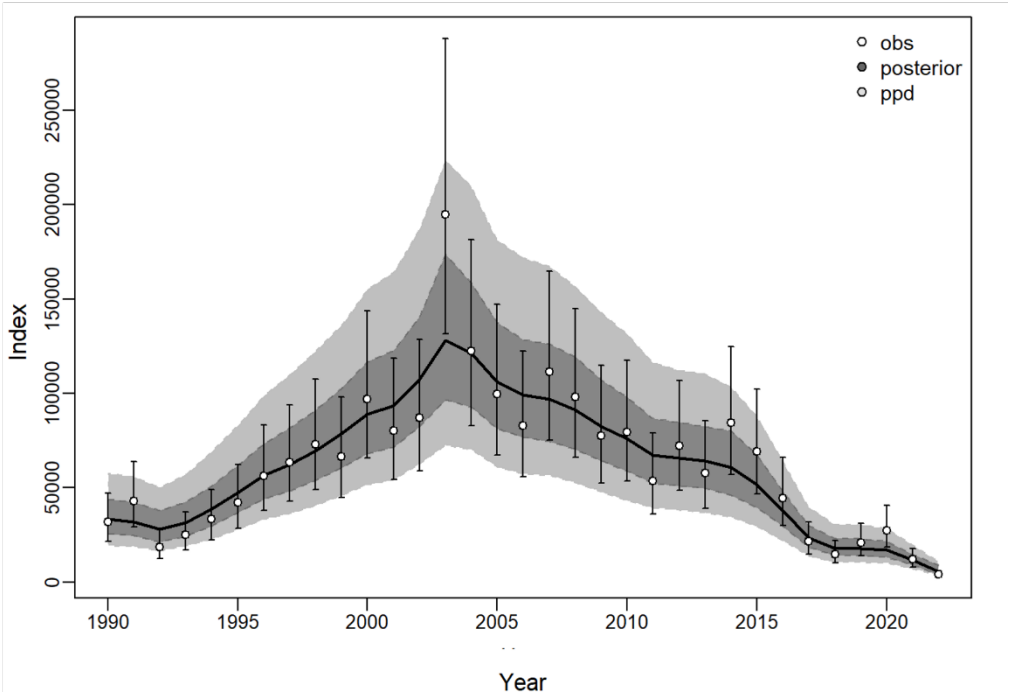

Figure 20. Total biomass index values observed for the Sept-Iles stock (white dots and associated error bars) and the trajectory estimated by the base model (black line). The shaded areas represent the posterior distribution of the predicted values (dark grey) and the predictive posterior distribution (PPD) (light grey).

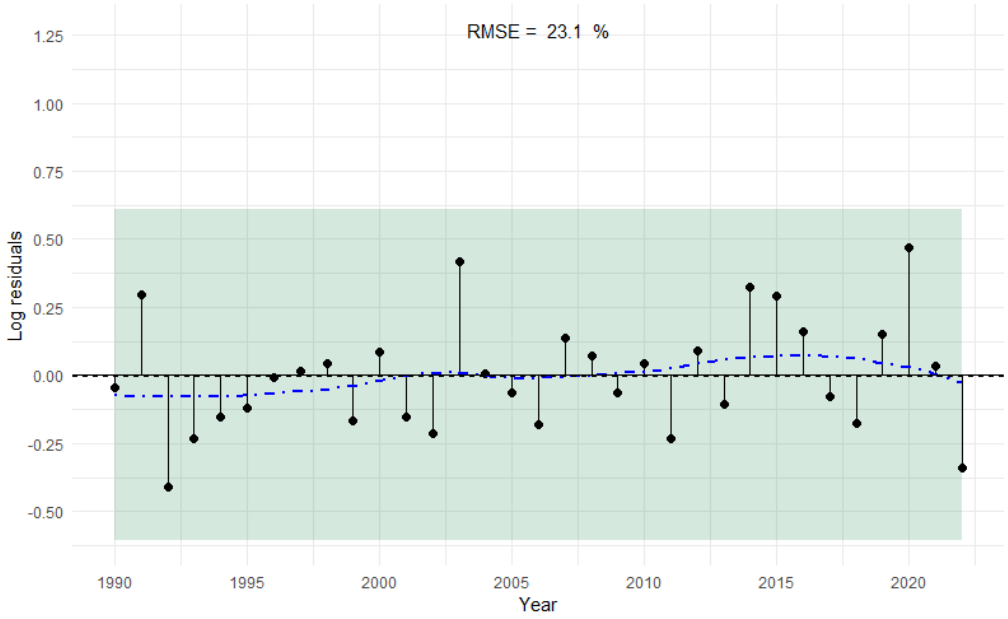

Figure 21. Residual diagnostics for the base model for the Sept-Iles stock, plotted on a log scale of biomass index values. The dot-dash blue line represents the LOESS-smoothed residuals, while the green background represents the results of the Wald-Wolfowitz test. The RMSE corresponds to the mean absolute error in percentage terms.

Sept-Iles

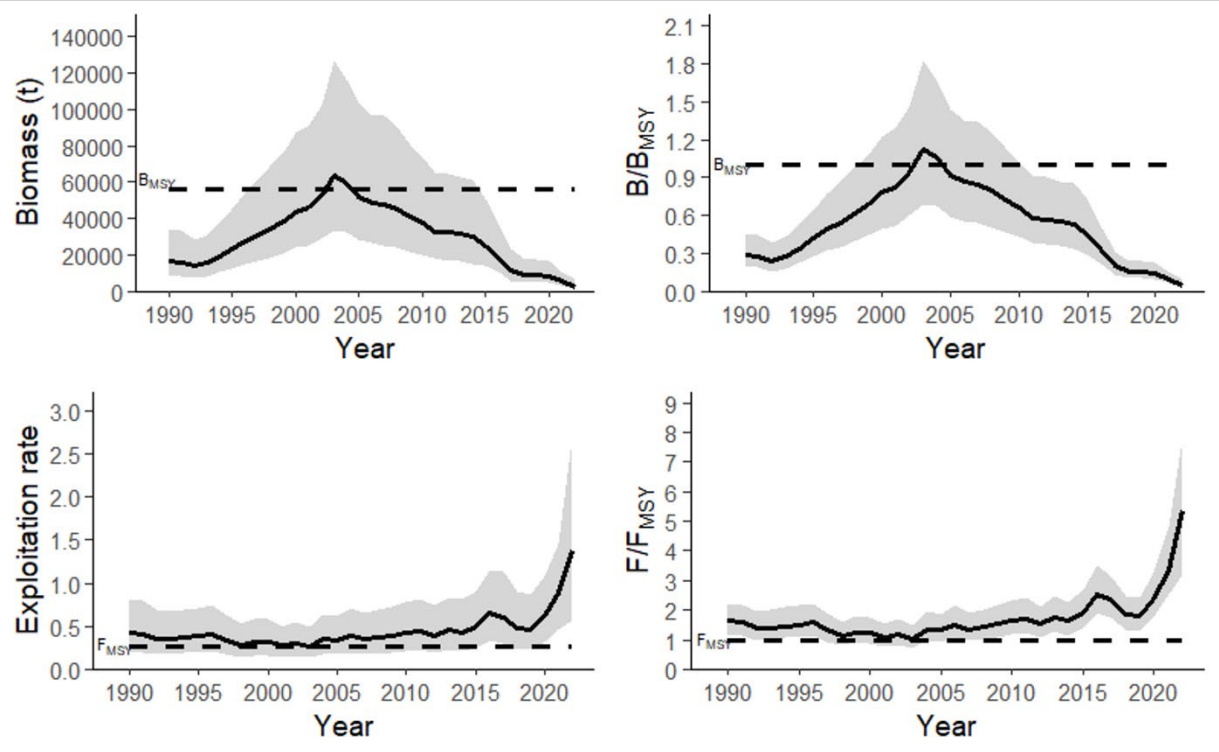

Figure 22. Estimated trajectories for Sept-Iles stock biomass (B_t) and fishing mortality (F_t), scaled according to the maximum sustainable yield (B/B_{MSY} and F/F_{MSY}). The shaded area represents the 95% confidence interval.

Sept-Îles

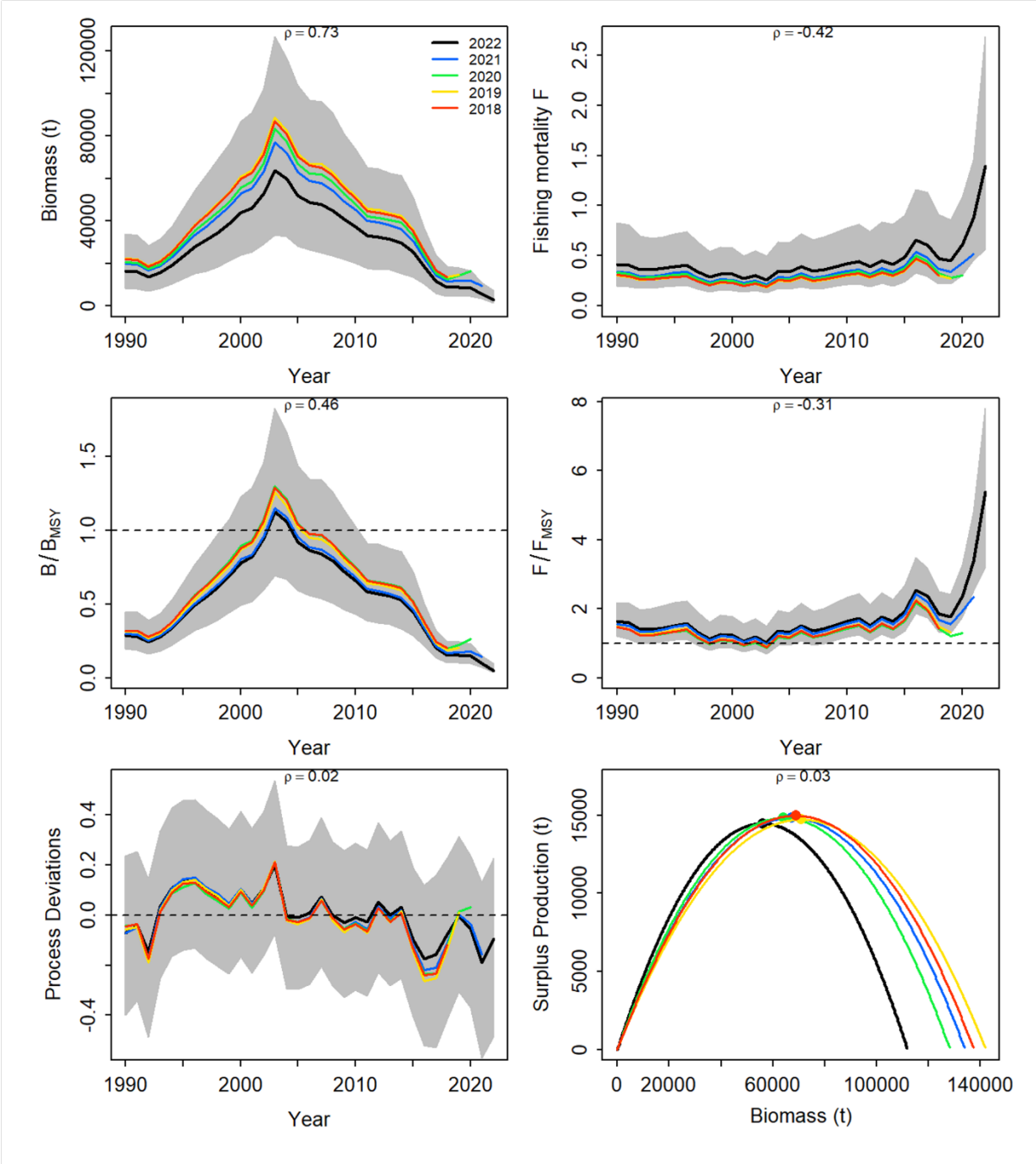

Figure 23. Retrospective analysis for the Sept-Iles stock (2018–2022). The mean Mohn's rho values are shown on each graph.

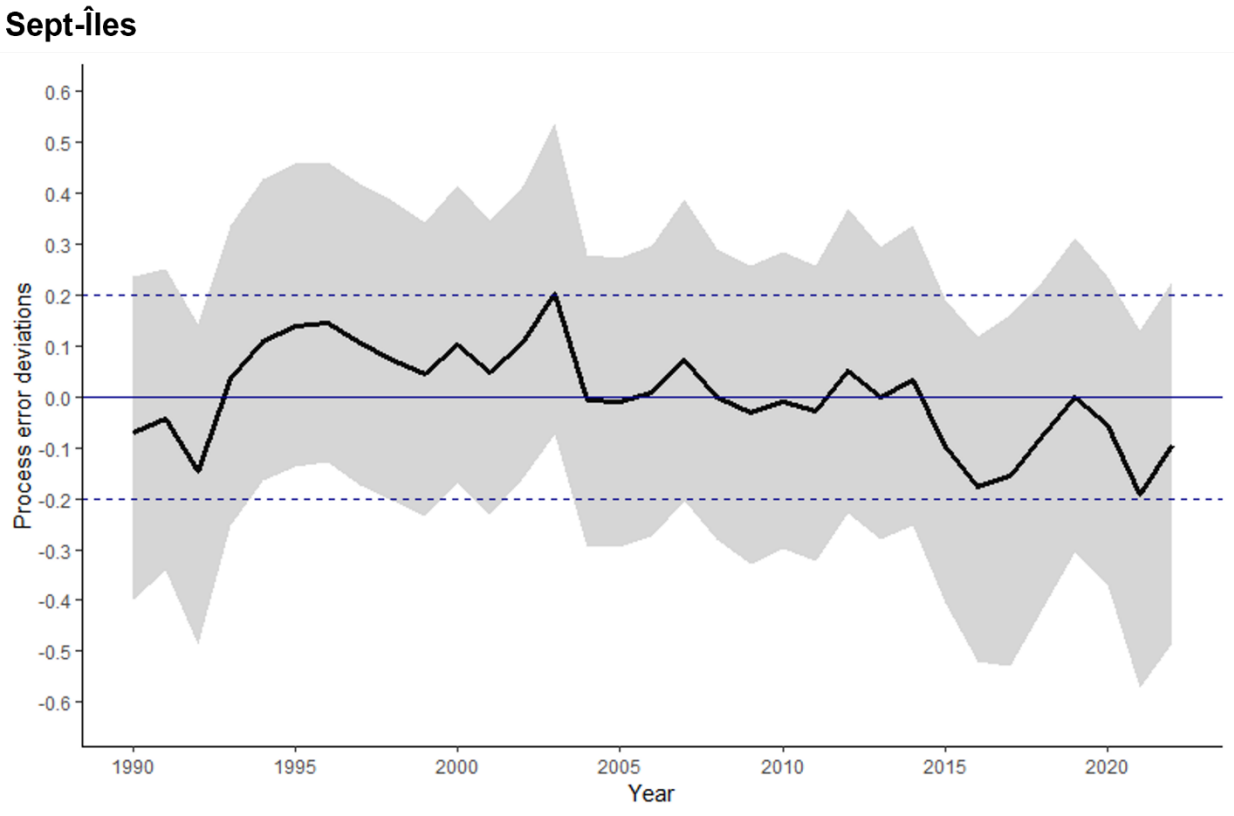

Figure 24. Process error deviation in the Sept-Iles model. The black line represents the median value of the posterior distribution, while the 95% CI is shown in grey. The solid blue line represents the trend for biomass generated by the deterministic portion of the model, while the dashed blue lines are provided to make the graph easier to read.

Sept-Îles

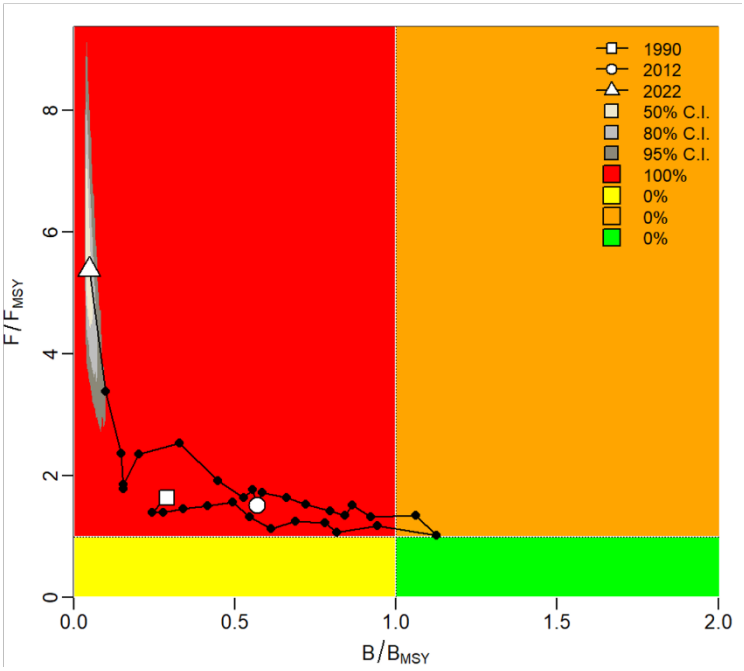

Figure 25. Kobe-type plot for the base case scenario for the Sept-Iles stock. The black line shows the estimated trajectory (1990–2022) between F/F_{MSY} and B/B_{MSY}. The grey shaded areas show the confidence intervals for the terminal year (50%, 80% and 95%). The probabilities of the terminal year being located in one of the quadrants are indicated in the legend.

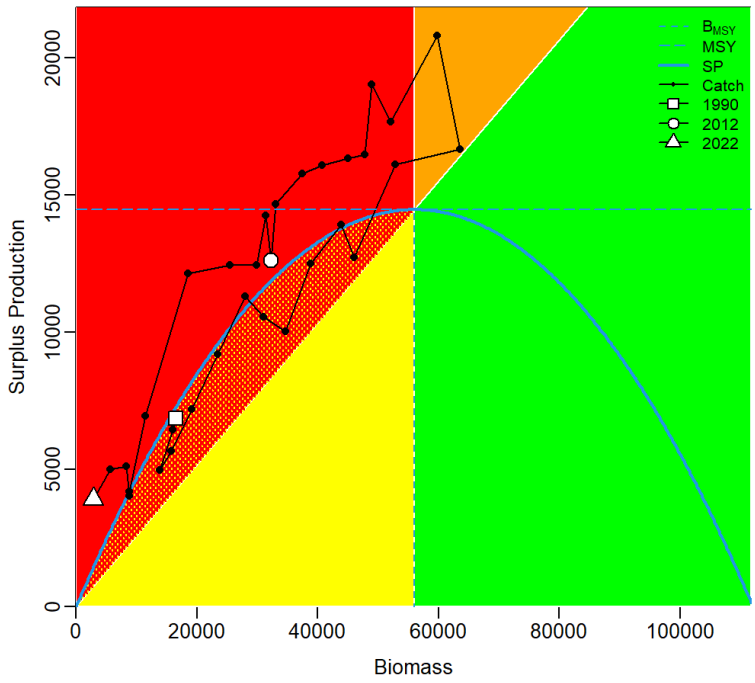

Figure 26. SP-phase-type plot showing the estimated surplus production curve (blue line) and the catch trajectory (black line) as a function of biomass for the base case scenario for the Sept-Iles stock. The blue dashed lines show the estimated values for maximum sustainable yield.

Estuary

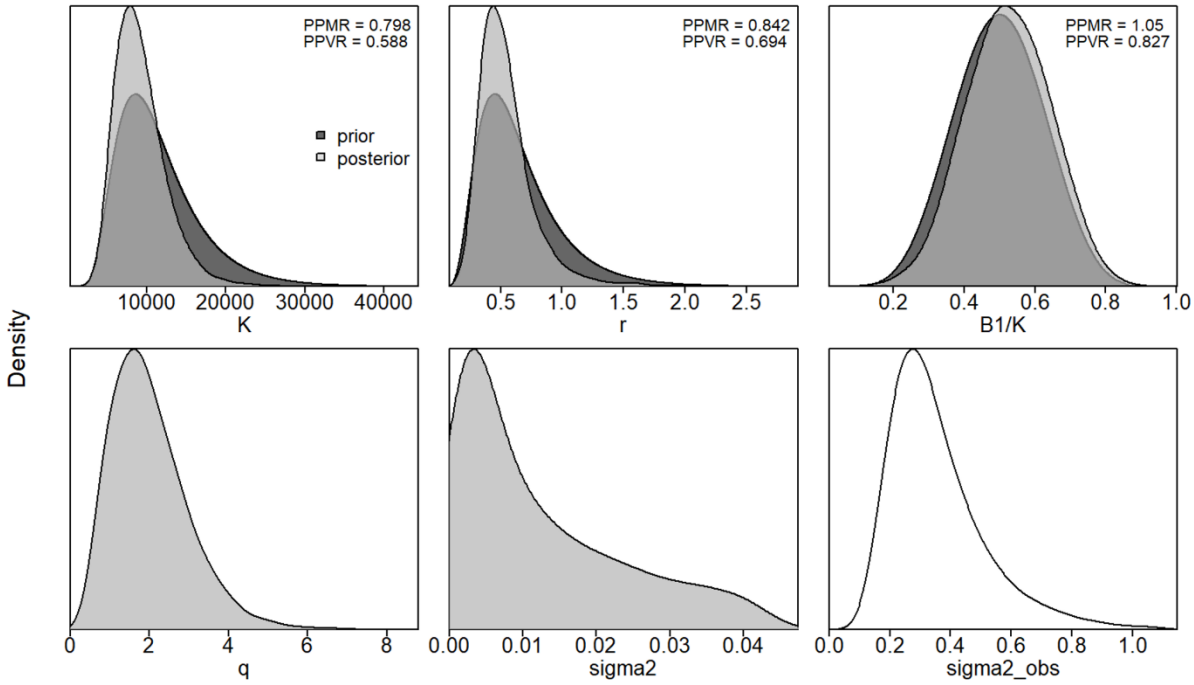

Figure 27. Prior distributions (dark grey) and posterior distributions (light grey) of the parameters used in the base model for Estuary. The parameters examined include carrying capacity (K), intrinsic rate of increase (r), biomass as a proportion of carrying capacity in the first year of the time series (B_1/K), the biomass index catchability coefficient (q), the process error variance σ_η^2 (sigma2) and the observation error variance $\sigma_{\varepsilon,t}^2$ (sigma2_obs). Posterior distributions were plotted using generic kernel densities.

Estuary

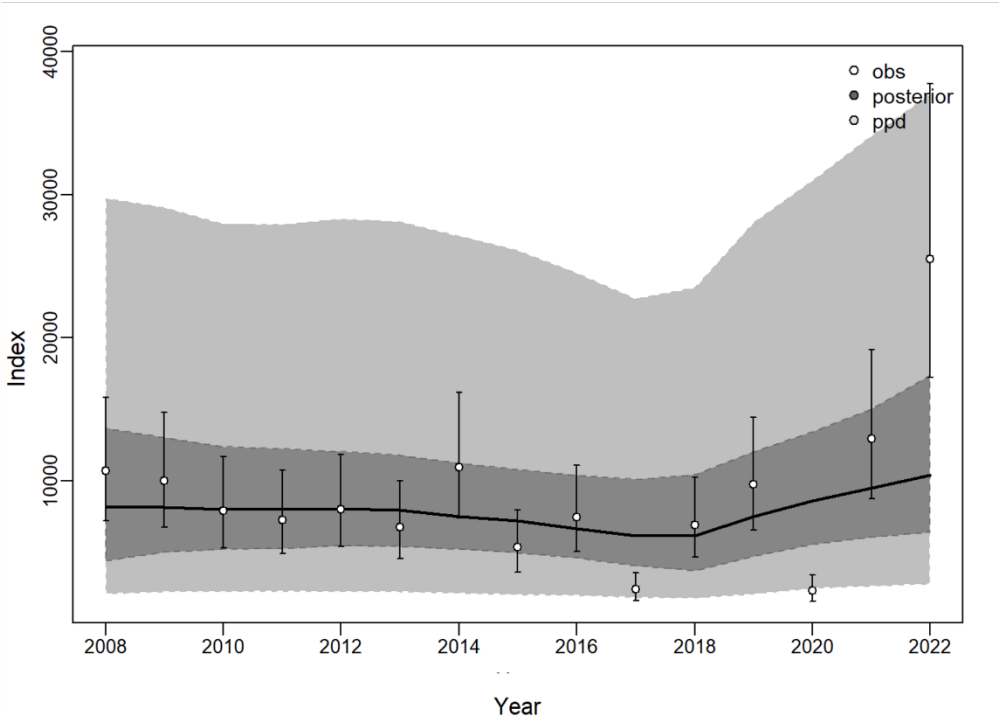

Figure 28. Total biomass index values observed for the Estuary stock (white dots and associated error bars) and the trajectory estimated by the base model (black line). The shaded areas represent the posterior distribution of the predicted values (dark grey) and the predictive posterior distribution (PPD) (light grey).

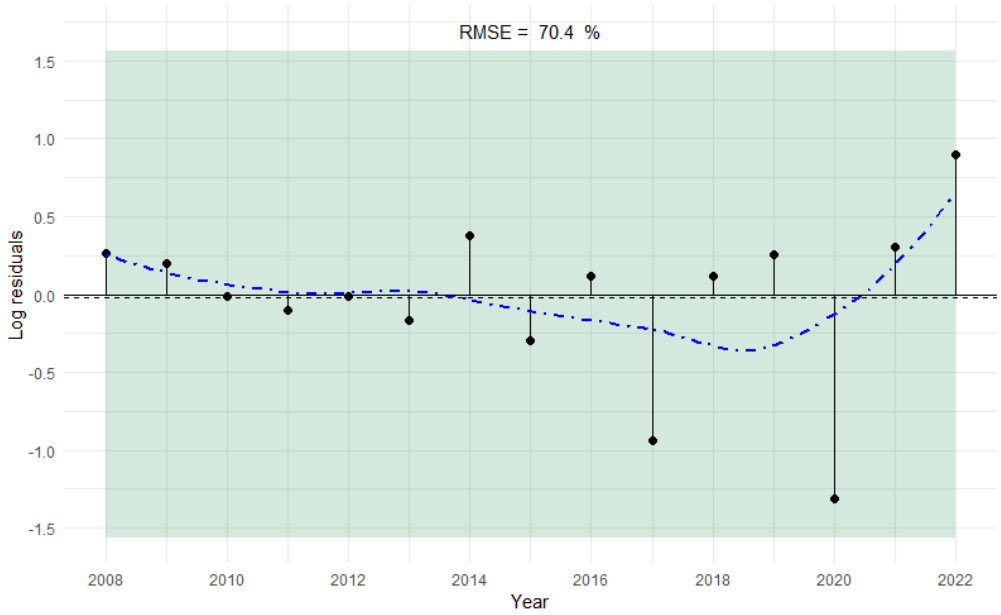

Figure 29. Residual diagnostics for the base model for the Estuary stock, plotted on a log scale of biomass index values. The dot-dash blue line represents the LOESS-smoothed residuals, while the green background represents the results of the Wald-Wolfowitz test. The RMSE corresponds to the mean absolute error in percentage terms.

Estuary

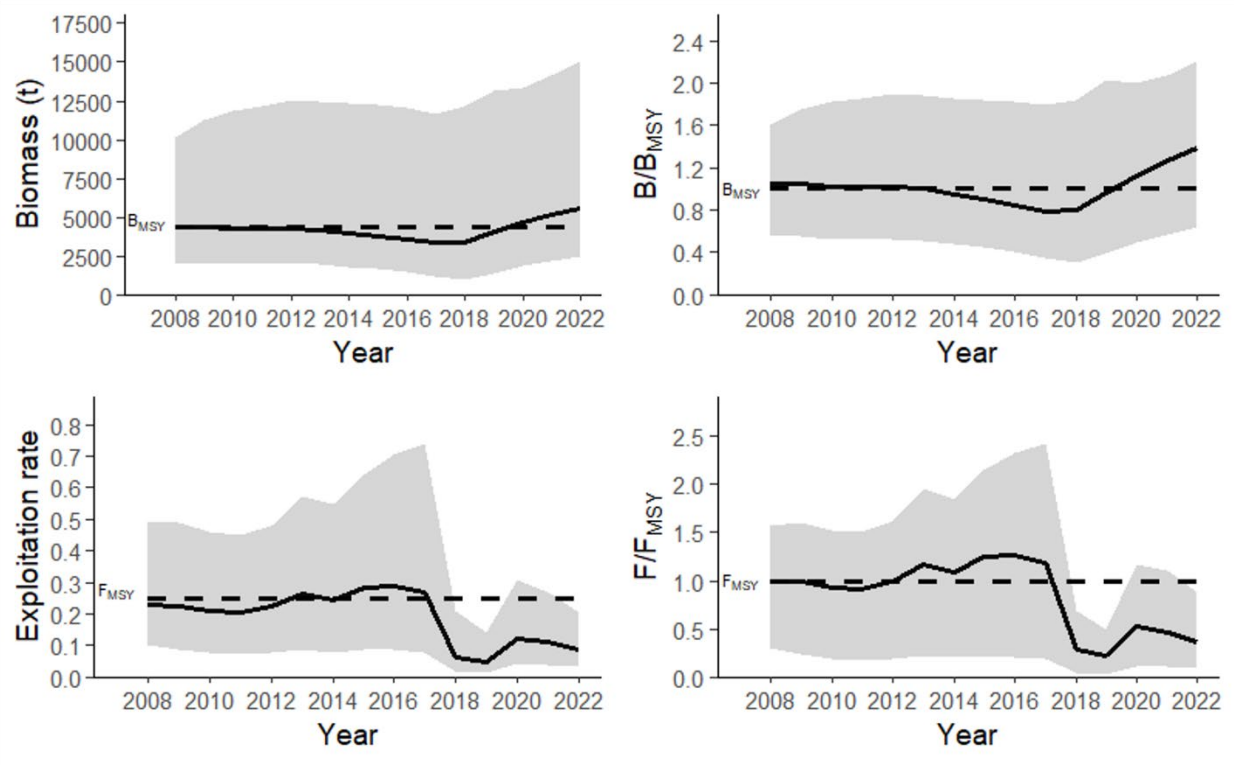

Figure 30. Estimated trajectories for Estuary stock biomass (B_t) and fishing mortality (F_t), scaled according to the maximum sustainable yield (B/B_{MSY} and F/F_{MSY}). The shaded area represents the 95% confidence interval.

Estuary

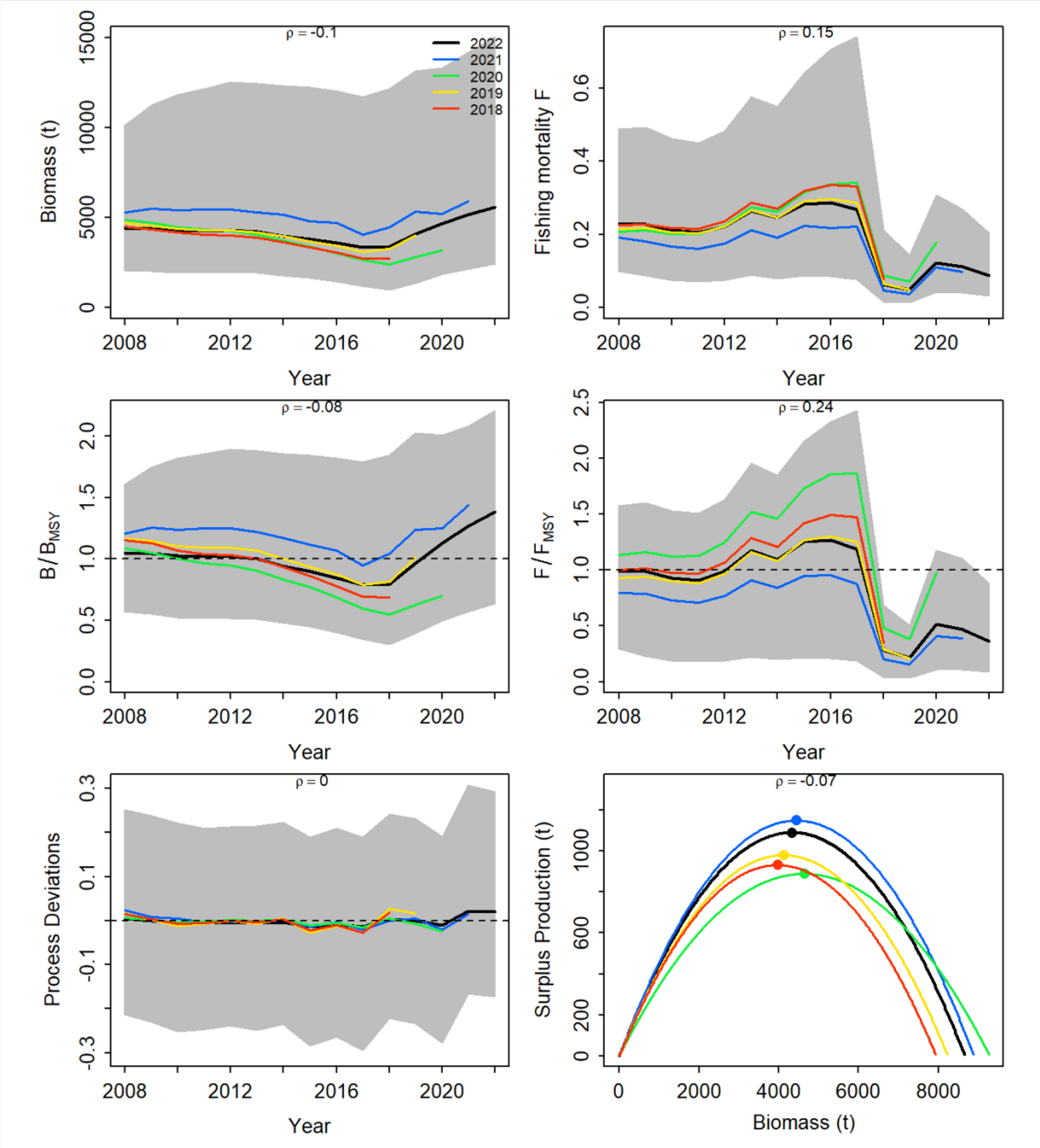

Figure 31. Retrospective analysis for the Estuary stock (2018–2022). The mean Mohn's rho values are shown on each graph.

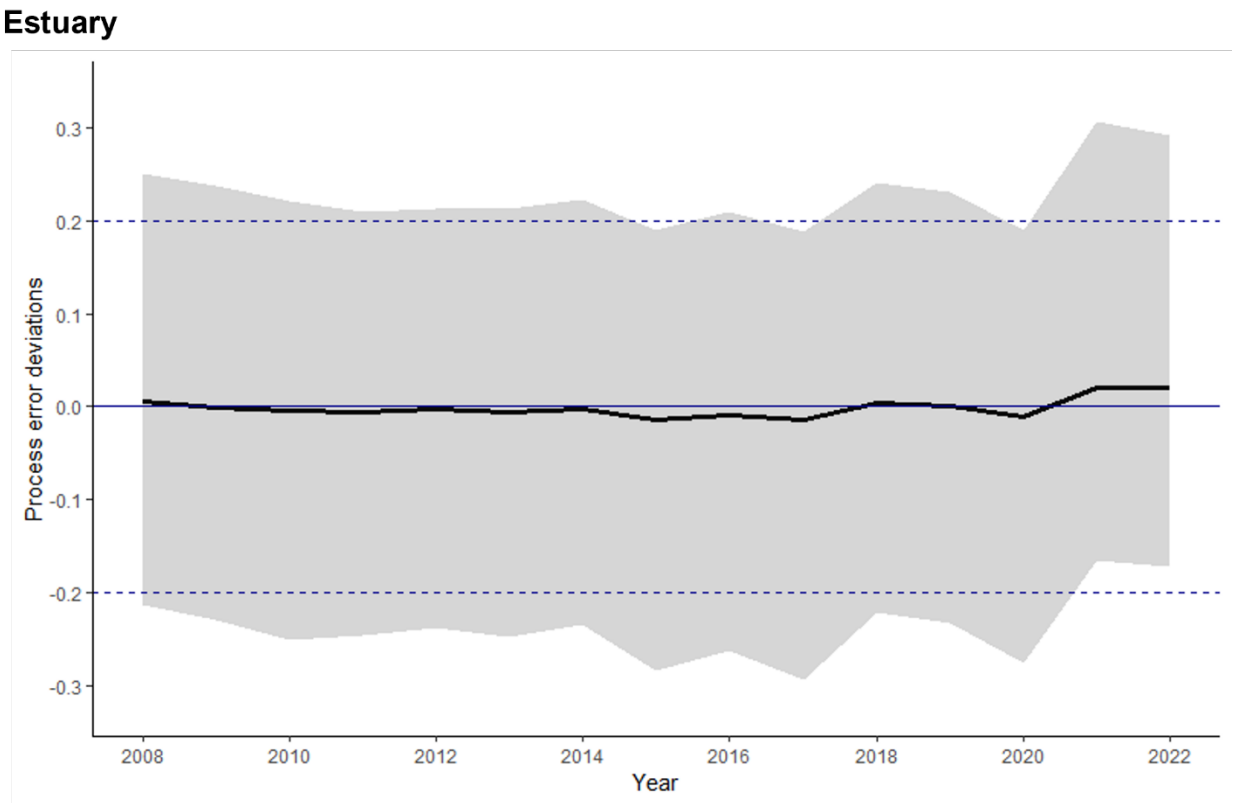

Figure 32. Process error deviation in the Estuary model. The black line represents the median value of the posterior distribution, while the 95% CI is shown in grey. The solid blue line represents the trend for biomass generated by the deterministic portion of the model, while the dashed blue lines are provided to make the graph easier to read.

Estuary

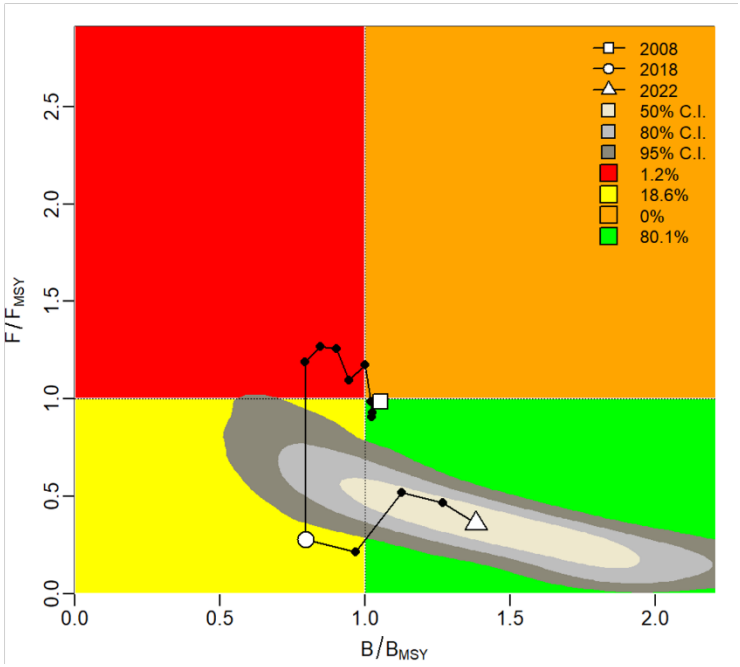

Figure 33. Kobe-type plot for the base case scenario for the Estuary stock. The black line shows the estimated trajectory (2008–2022) between F/F_{MSY} and B/B_{MSY}. The grey shaded areas show the confidence intervals for the terminal year (50%, 80% and 95%). The probabilities of the terminal year being located in one of the quadrants are indicated in the legend.

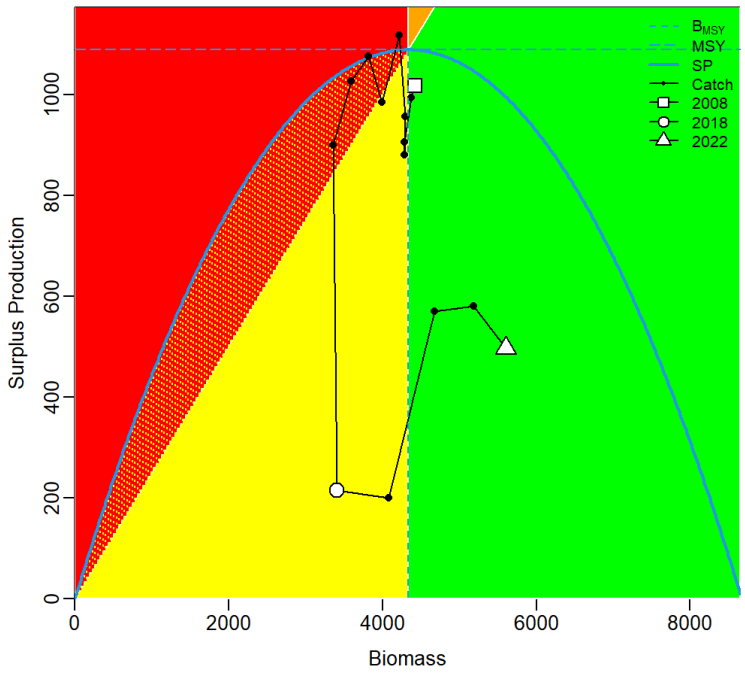

Figure 34. SP-phase-type plot showing the estimated surplus production curve (blue line) and the catch trajectory (black line) as a function of biomass for the base case scenario for the Estuary stock. The blue dashed lines show the estimated values for maximum sustainable yield.

Esquiman

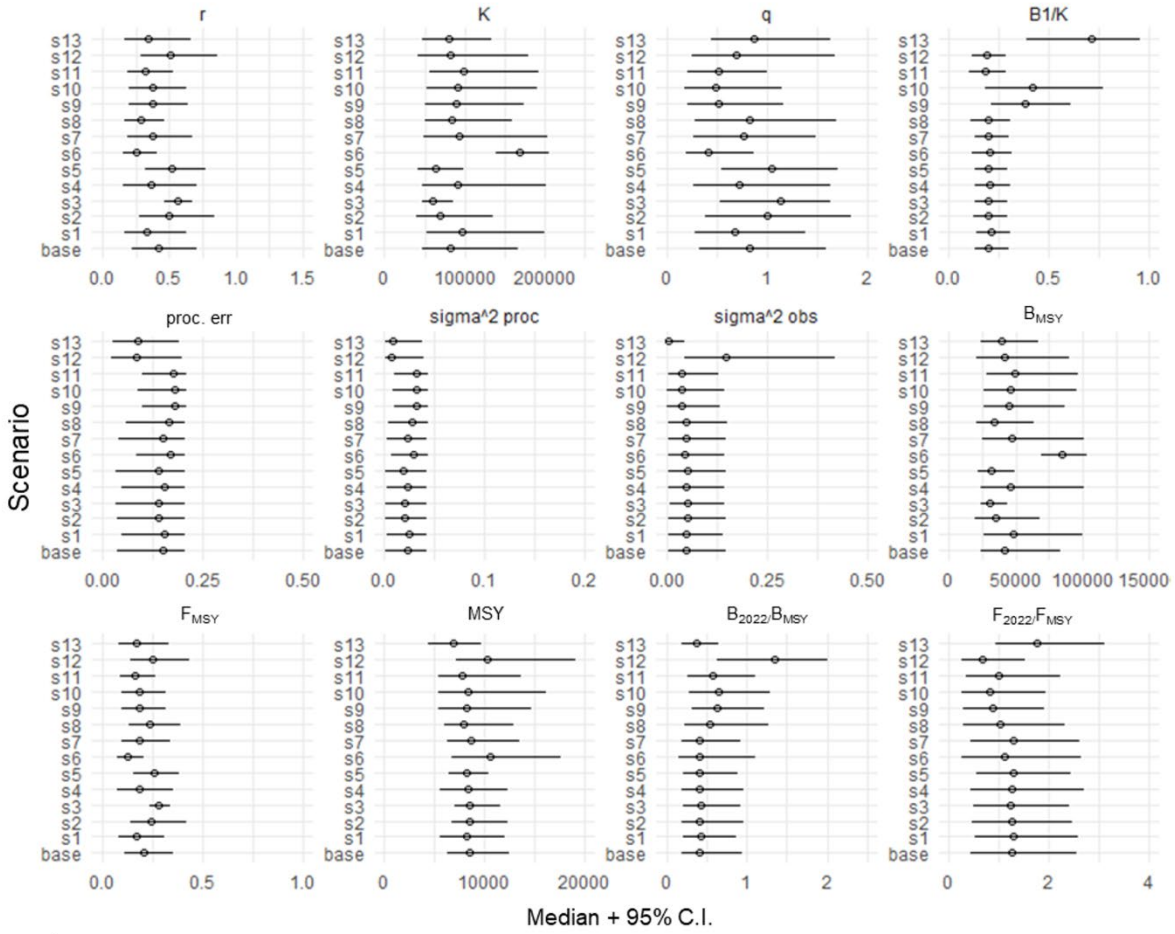

Legend

ID	Scenario	ID	Scenario
base	base	s7	K_sd_high
s1	r_low	s8	$B_{RMD}/K = 0.4$
s2	r_high	s9	$B_1/K = 0.5$
s3	r_sd_low	s10	$B_1/K = 0.7$
s4	r_sd_high	s11	1982-2022
s5	K_low	s12	1990-2005
s6	K_high	s13	2005-2022

Figure 35. Posterior distributions for the various parameters estimated and derived by the model according to the different sensitivity tests compared with the base model for the Esquiman stock. The points represent median values and the horizontal lines, the 95% CI. The various scenarios (s) are described in the legend. The distributions shown include the intrinsic rate of increase (r), carrying capacity (K), catchability coefficient (q), biomass as a proportion of carrying capacity in the first year of the time series (B_1/K), process error variance σ_η and σ_η^2 (process error and sigma^2 proc respectively), estimated observation error variance σ_{est}^2 (sigma^2 obs), biomass at MSY (B_{MSY}), exploitation rate at MSY (F_{MSY}), maximum sustainable yield (MSY), and lastly the relative biomass and relative exploitation rate in the terminal year (t) (B_t/B_{MSY} and F_t/F_{MSY} respectively). See the text for more details.

Esquiman

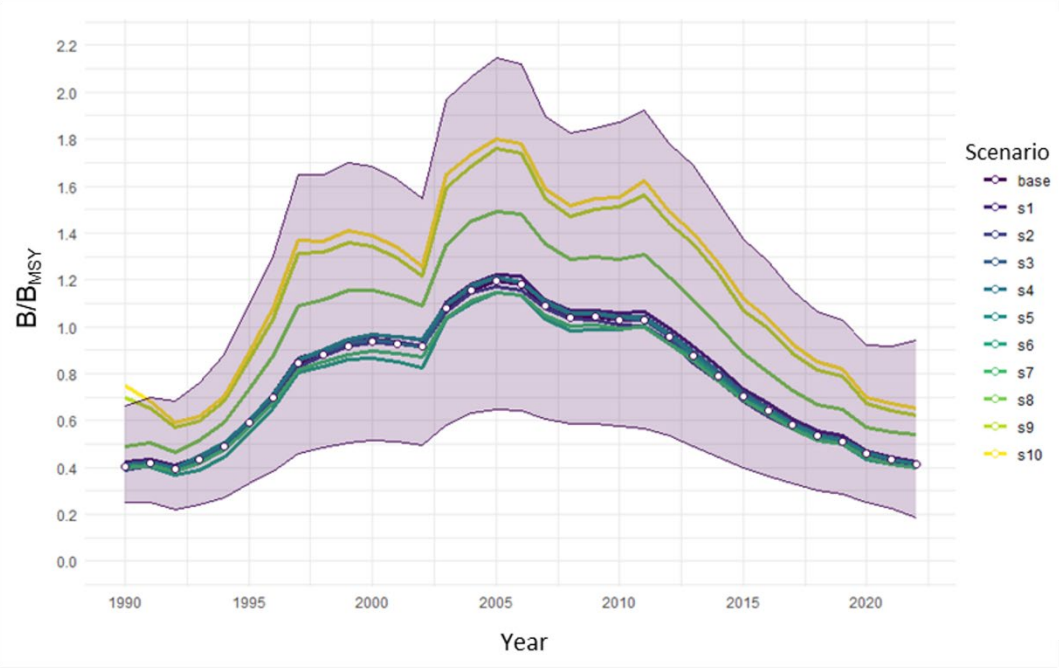

Legend

ID	Scenario	ID	Scenario
base	base	s7	K_sd_high
s1	r_low	s8	$B_{RMD}/K = 0.4$
s2	r_high	s9	$B_1/K = 0.5$
s3	r_sd_low	s10	$B_1/K = 0.7$
s4	r_sd_high		
s5	K_low		
s6	K_high		

Figure 36. Comparison of B/B_{MSY} trajectories in the base model (line with white dots and 95% CI) and sensitivity tests s1–s10 (coloured lines) for the Esquiman stock.

Anticosti

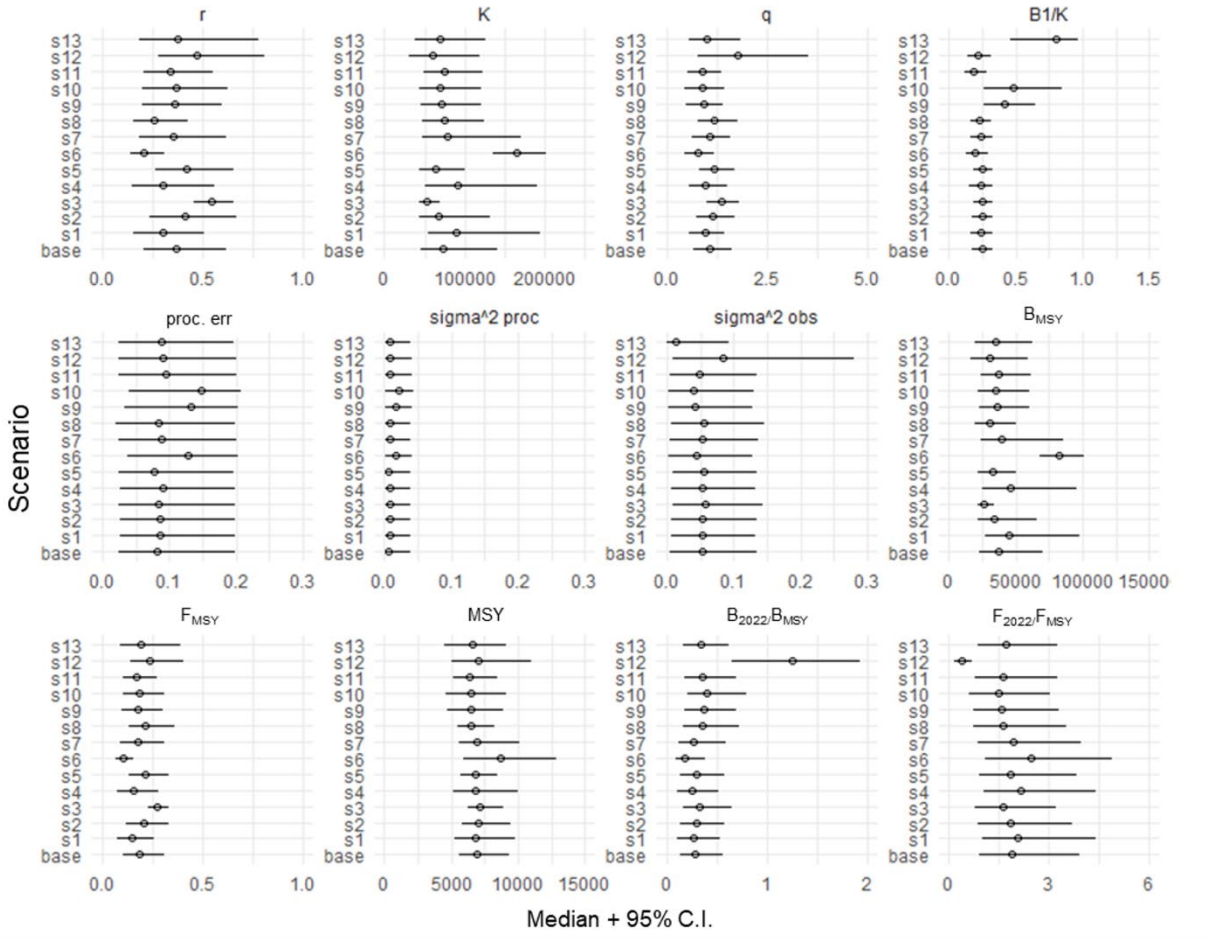

Legend

ID	Scenario	ID	Scenario
base	base	s7	K_sd_high
s1	r_low	s8	$B_{RMD}/K = 0.4$
s2	r_high	s9	$B_1/K = 0.5$
s3	r_sd_low	s10	$B_1/K = 0.7$
s4	r_sd_high	s11	1982-2022
s5	K_low	s12	1990-2005
s6	K_high	s13	2005-2022

Figure 37. Posterior distributions for the various parameters estimated and derived by the model according to the different sensitivity tests compared with the base model for the Anticosti stock. The points represent median values and the horizontal lines, the 95% CI. The various scenarios (s) are described in the legend. The distributions shown include the intrinsic rate of increase (r), carrying capacity (K), catchability coefficient (q), biomass as a proportion of carrying capacity in the first year of the time series (B_1/K), process error variance σ_η and σ_η^2 (process error and sigma^2 proc respectively), estimated observation error variance σ_{est}^2 (sigma^2 obs), biomass at MSY (B_{MSY}), exploitation rate at MSY (F_{MSY}), maximum sustainable yield (MSY), and lastly the relative biomass and relative exploitation rate in the terminal year (t) (B_t/B_{MSY} and F_t/F_{MSY} respectively). See the text for more details.

Anticosti

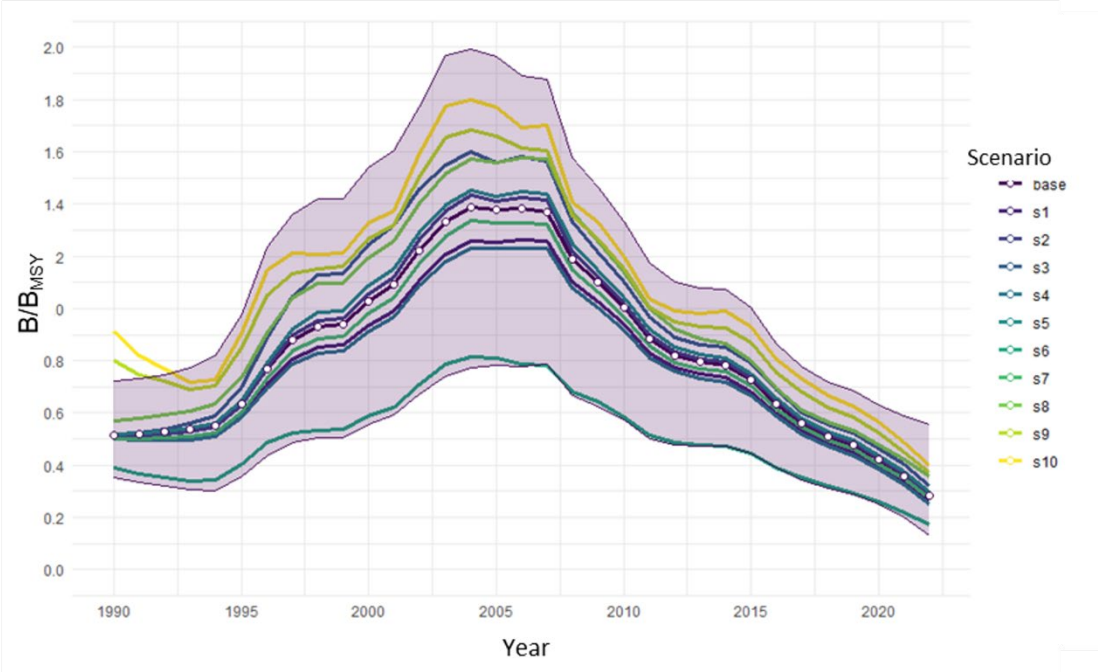

Legend

ID	Scenario	ID	Scenario
base	base	s7	K_sd_high
s1	r_low	s8	$B_{RMD}/K = 0.4$
s2	r_high	s9	$B_1/K = 0.5$
s3	r_sd_low	s10	$B_1/K = 0.7$
s4	r_sd_high		
s5	K_low		
s6	K_high		

Figure 38. Comparison of B/B_{MSY} trajectories in the base model (line with white dots and 95% CI) and sensitivity tests s1–s10 (coloured lines) for the Anticosti stock.

Sept-Iles

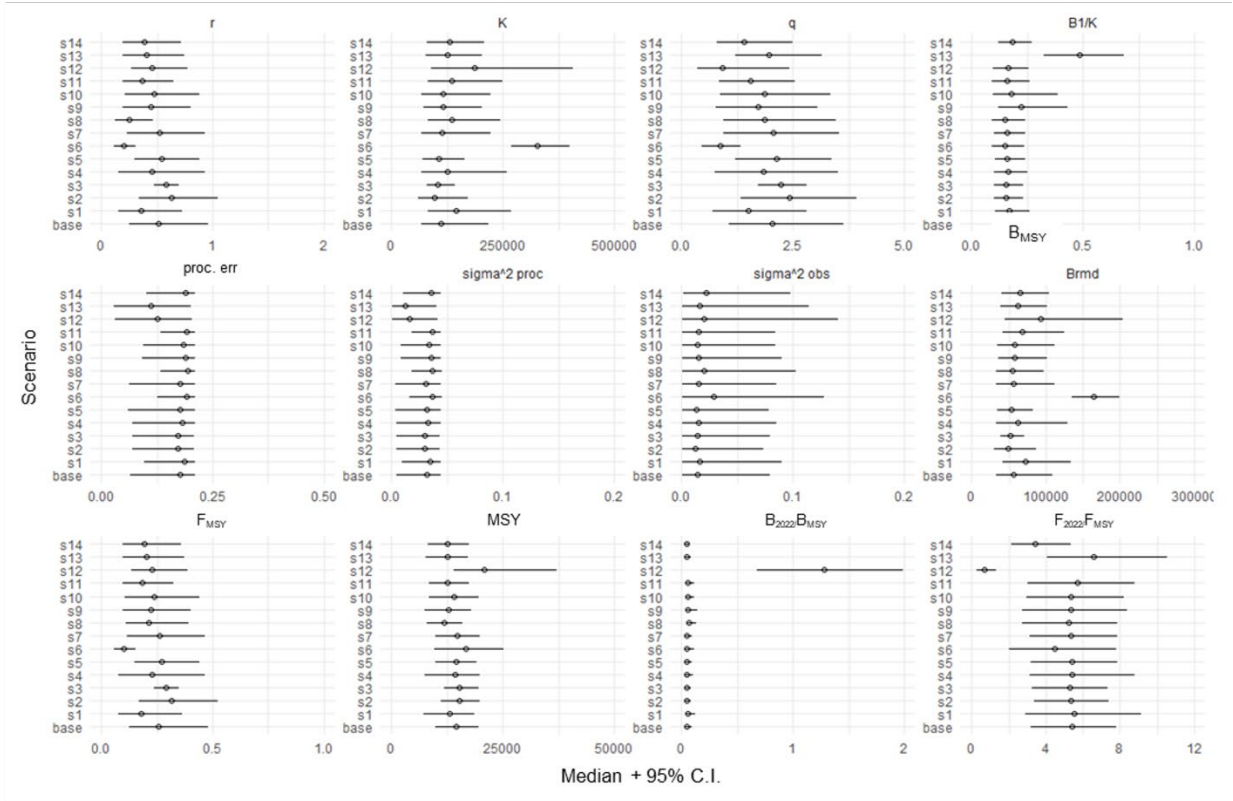

Legend

ID	Scenario	ID	Scenario
base	base	s7	K_sd_high
s1	r_low	s8	B_{RMD}/K = 0.4
s2	r_high	s9	B_1/K = 0.5
s3	r_sd_low	s10	B_1/K =0.7
s4	r_sd_high	s11	1982-2022
s5	K_low	s12	1990-2005
s6	K_high	s13	2005-2022

Figure 39. Posterior distributions for the various parameters estimated and derived by the model according to the different sensitivity tests compared with the base model for the Sept-Iles stock. The points represent median values and the horizontal lines, the 95% CI. The various scenarios (s) are described in the legend. The distributions shown include the intrinsic rate of increase (r), carrying capacity (K), catchability coefficient (q), biomass as a proportion of carrying capacity in the first year of the time series (B_1/K), process error variance σ_η and σ_η^2 (process error and sigma^2 proc respectively), estimated observation error variance σ_{est}^2 (sigma^2 obs), biomass at MSY (B_{MSY}), exploitation rate at MSY (F_{MSY}), maximum sustainable yield (MSY), and lastly the relative biomass and relative exploitation rate in the terminal year (t) (B_t/B_{MSY} and F_t/F_{MSY} respectively). See the text for more details.

Sept-Iles

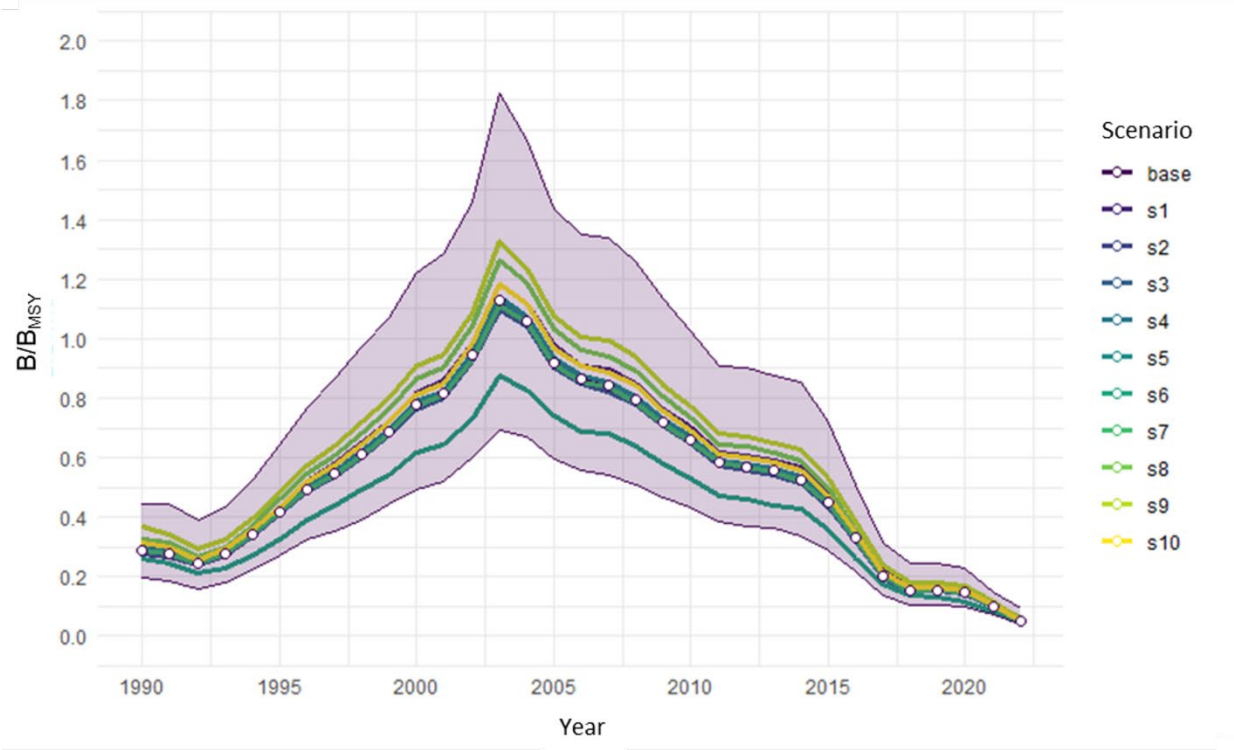

Legend

ID	Scenario	ID	Scenario
base	base	s7	K_sd_high
s1	r_low	s8	$B_{RMD}/K = 0.4$
s2	r_high	s9	$B_1/K = 0.5$
s3	r_sd_low	s10	$B_1/K = 0.7$
s4	r_sd_high		
s5	K_low		
s6	K_high		

Figure 40. Comparison of B/B_{MSY} trajectories in the base model (line with white dots and 95% CI) and sensitivity tests s1–s10 (coloured lines) for the Sept-Iles stock.

Estuary

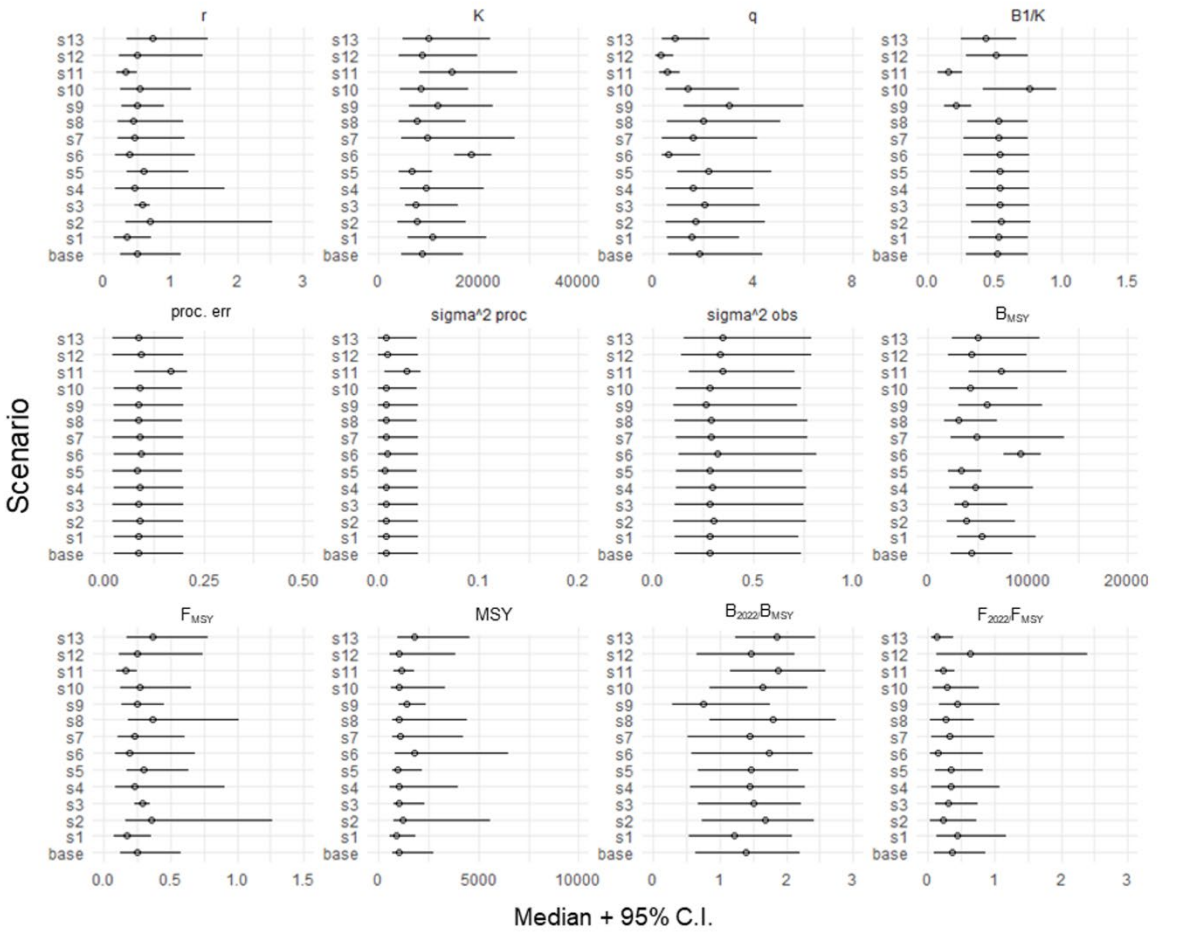

Legend

ID	Scenario	ID	Scenario
base	base	s7	K_sd_high
s1	r_low	s8	$B_{RMD}/K = 0.4$
s2	r_high	s9	$B_1/K = 0.5$
s3	r_sd_low	s10	$B_1/K = 0.7$
s4	r_sd_high	s11	1982-2022
s5	K_low	s12	1990-2005
s6	K_high	s13	2005-2022

Figure 41. Posterior distributions for the various parameters estimated and derived by the model according to the different sensitivity tests compared with the base model for the Estuary stock. The points represent median values and the horizontal lines, the 95% CI. The various scenarios (s) are described in the legend. The distributions shown include the intrinsic rate of increase (r), carrying capacity (K), catchability coefficient (q), biomass as a proportion of carrying capacity in the first year of the time series (B_1/K), process error variance σ_η and σ_η^2 (process error and sigma^2 proc respectively), estimated observation error variance σ_{est}^2 (sigma^2 obs), biomass at MSY (B_{MSY}), exploitation rate at MSY (F_{MSY}), maximum sustainable yield (MSY), and lastly the relative biomass and relative exploitation rate in the terminal year (t) (B_t/B_{MSY} and F_t/F_{MSY} respectively). See the text for more details.

Estuary

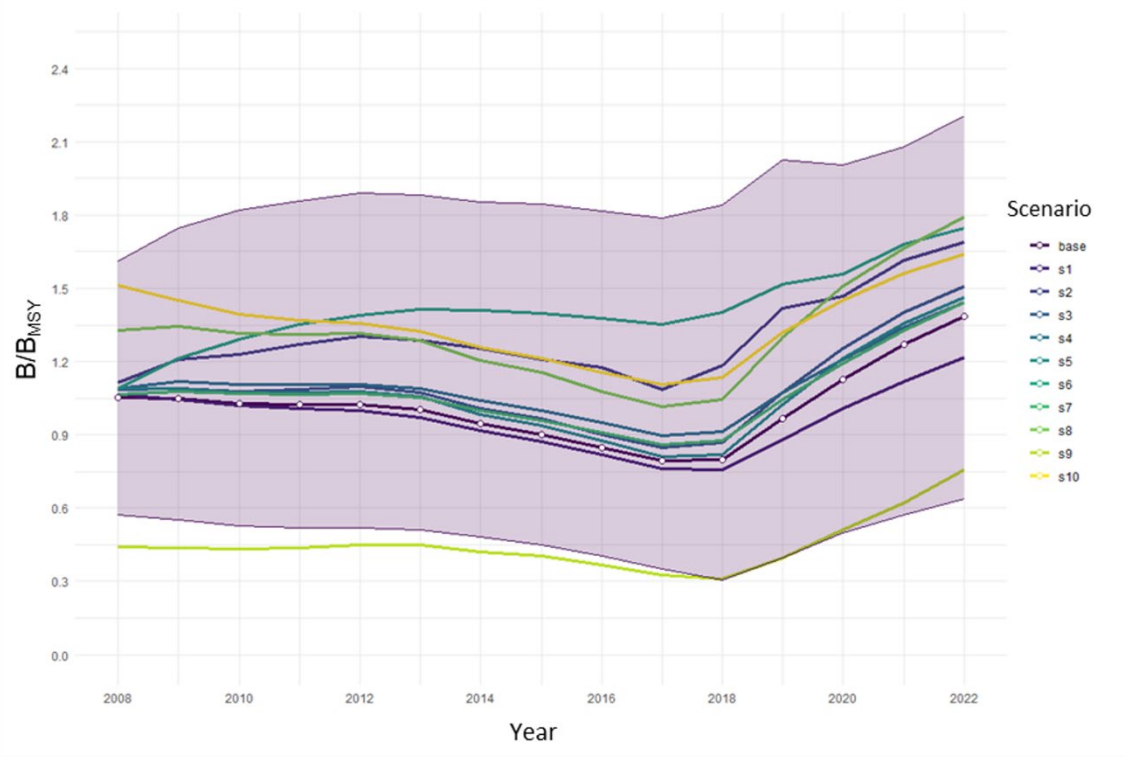

Legend

ID	Scenario	ID	Scenario
base	base	s7	K_sd_high
s1	r_low	s8	$B_{RMD}/K = 0.4$
s2	r_high	s9	$B_1/K = 0.5$
s3	r_sd_low	s10	$B_1/K = 0.7$
s4	r_sd_high		
s5	K_low		
s6	K_high		

Figure 42. Comparison of B/B_{MSY} trajectories in the base model (line with white dots and 95% CI) and sensitivity tests s1–s10 (coloured lines) for the Estuary stock.

Esquiman

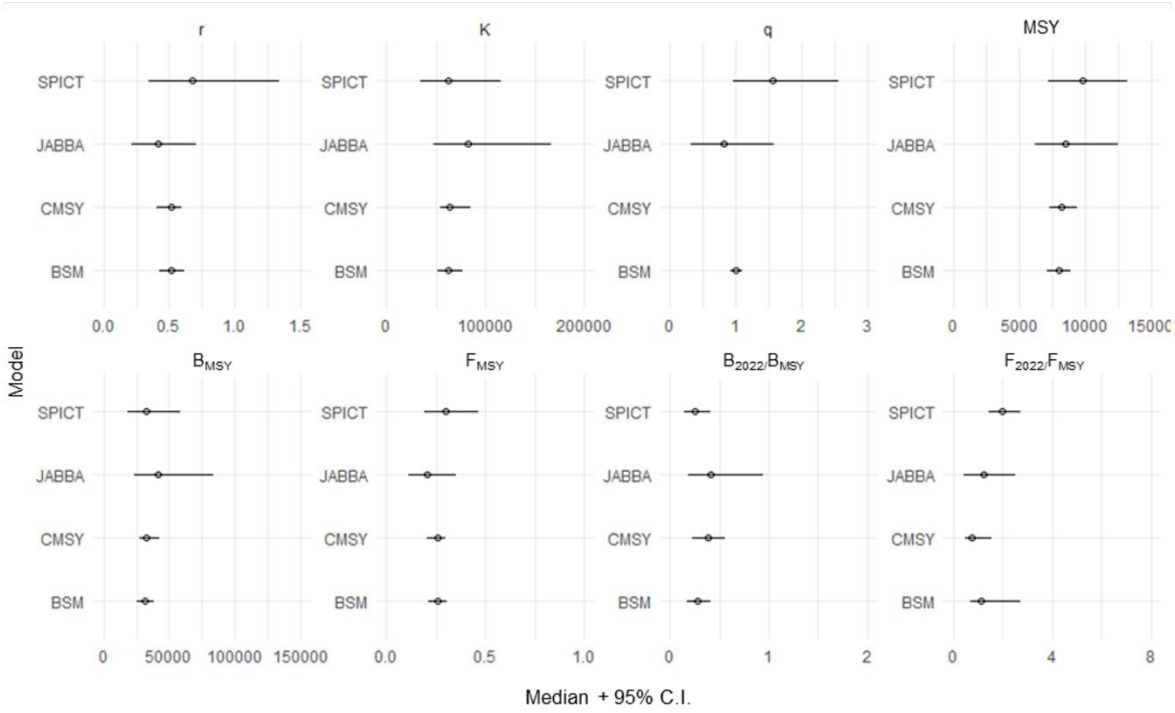

Figure 43. Posterior distributions of the various parameters for the Esquiman stock estimated by the model using the different sensitivity tests versus those provided by the base model.

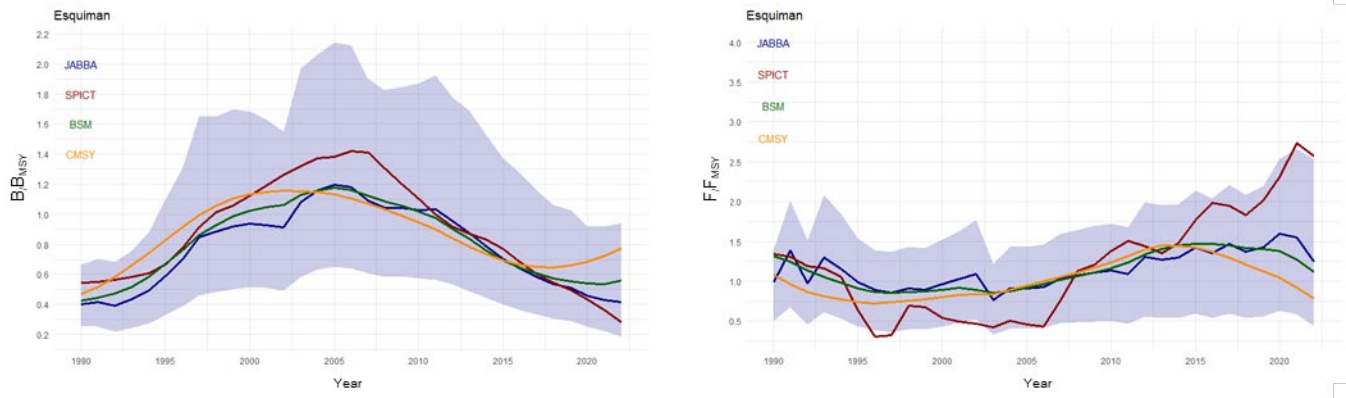

Figure 44. Comparison of the B/B_{MSY} and F/F_{MSY} trajectories provided by the JABBA base model for the Esquiman stock (blue line and shaded area for 95% CI) and those provided by the SPiCT, BSM and CMSY++ models.

Anticosti

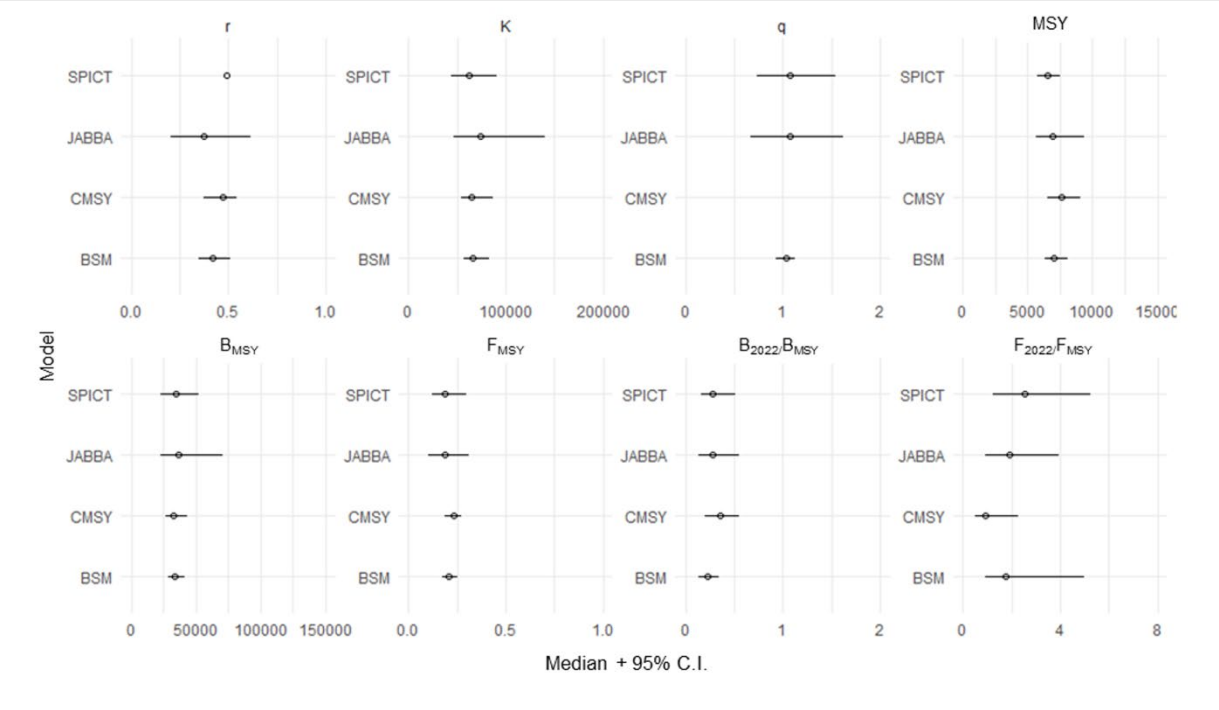

Figure 45. Posterior distributions of the various parameters for the Anticosti stock estimated by the model using the different sensitivity tests versus those provided by the base model.

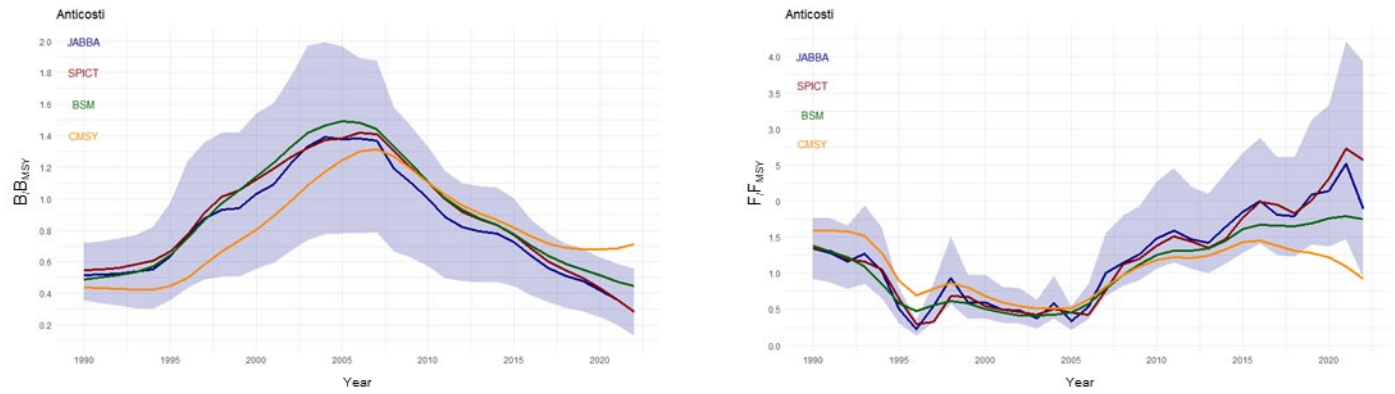

Figure 46. Comparison of the B/B_{MSY} and F/F_{MSY} trajectories provided by the JABBA base model for the Anticosti stock (blue line and shaded area for 95% CI) and those provided by the SPiCT, BSM and CMSY++ models.

Sept-Iles

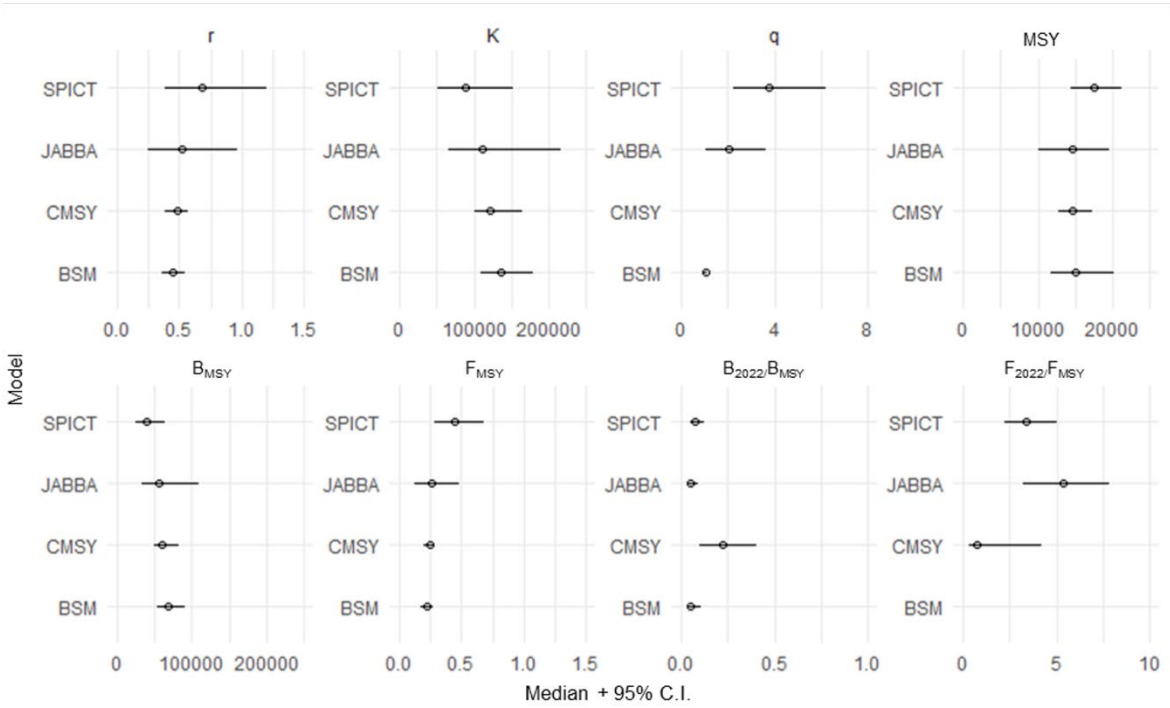

Figure 47. Posterior distributions of the various parameters for the Sept-Iles stock estimated by the model using the different sensitivity tests versus those provided by the base model.

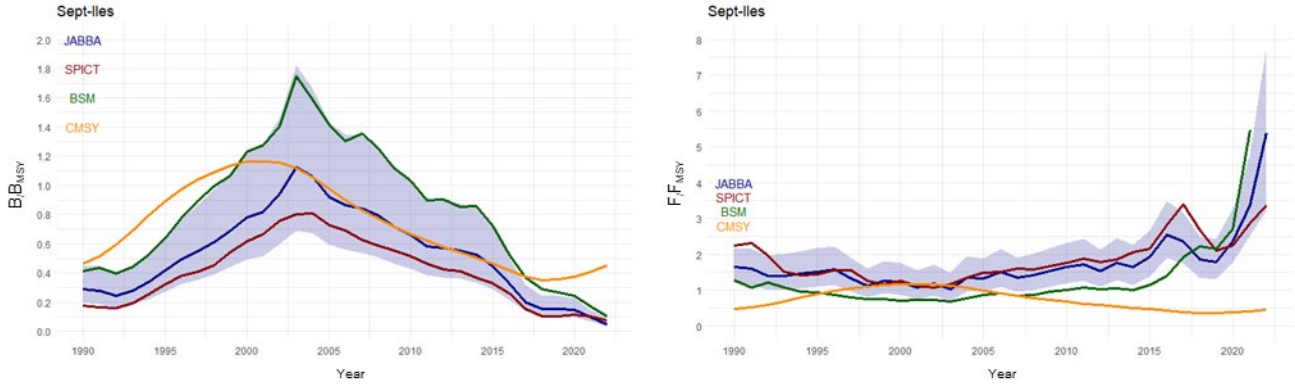

Figure 48. Comparison of the B/B_{MSY} and F/F_{MSY} trajectories provided by the JABBA base model for the Sept-Iles stock (blue line and shaded area for 95% CI) and those provided by the SPiCT, BSM and CMSY++ models.

Estuary

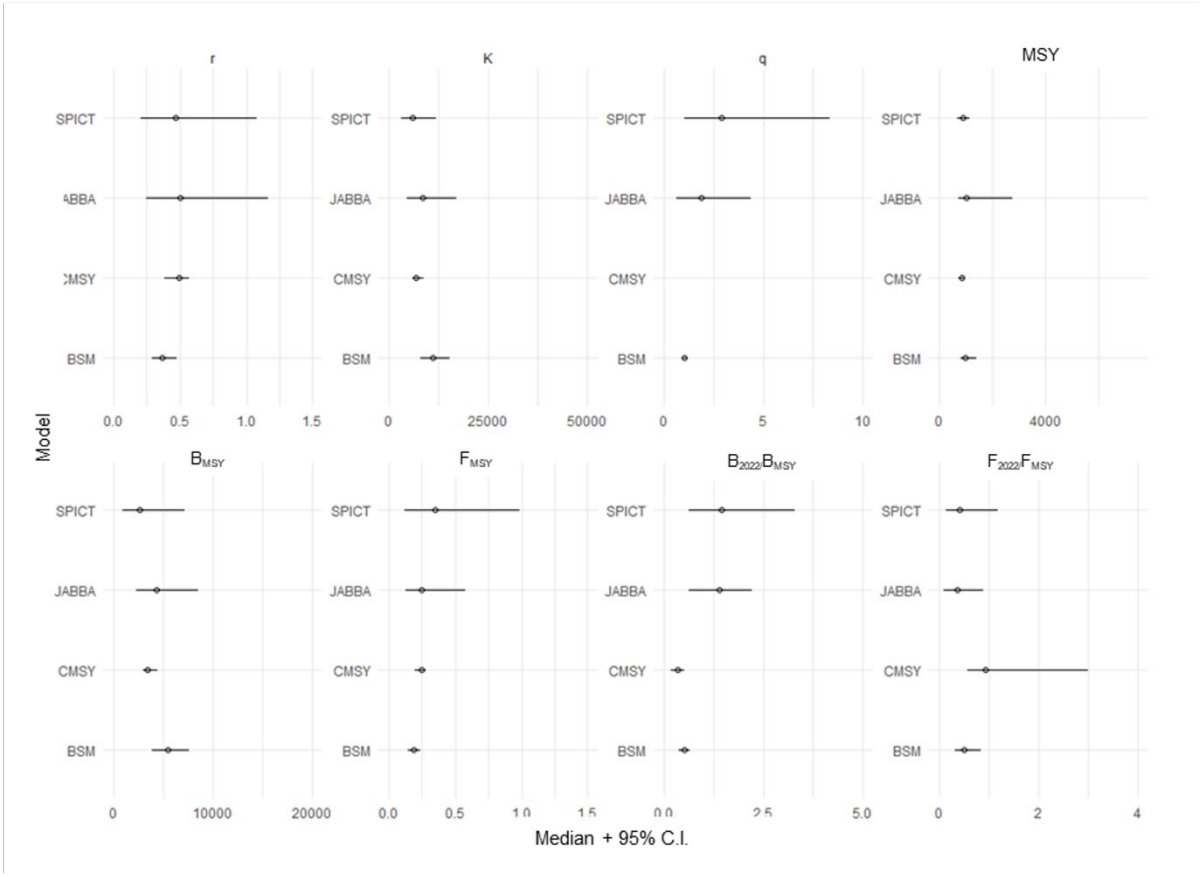

Figure 49. Posterior distributions of the various parameters for the Estuary stock estimated by the model using the different sensitivity tests versus those provided by the base model.

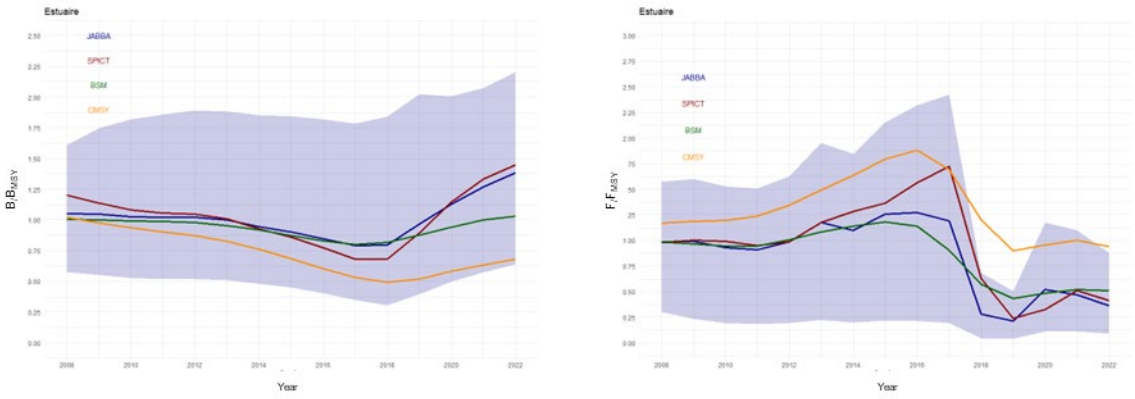

Figure 50. Comparison of the B/B_{MSY} and F/F_{MSY} trajectories provided by the JABBA base model for the Estuary stock (blue line and shaded area for 95% CI) and those provided by the SPiCT, BSM and CMSY++ models.